Low-variance parameter estimation approach for real-time optimization of noisy process systems

Gabriel D. Patrón[a], Luis Ricardez-Sandoval[a]*

[a]Department of Chemical Engineering, University of Waterloo, Waterloo, ON, Canada N2L 3G1

*Corresponding author: e-mail: laricard@uwaterloo.ca, phone: (+1) 519 888 4567 x38667, fax, (+1) 519 888 4347

Abstract

Uncertainty is inherent to the measurement and modelling of process systems, where it can have significant impacts on the efficacy of optimization techniques. This work proposes a scheme to address uncertainty as it pertains to real-time optimization (RTO), where noisy measurements are used to estimate model parameters and account for model uncertainty. The parameter estimation (PE) step that accompanies RTO requires plant measurements that are often noisy; this can cause the propagation of noise to the parameter estimates, which may result in poor RTO performance. An information content (IC) metric for choosing the most information-rich measurements, and an algorithm to select a favourable subset of measurements as well as filtering for erroneous parameters, are proposed in this work to improve the PE problem performance. The resulting low-variance PE (lv-PE) algorithm yields parameter estimates which are closer to the true parameter values over many RTO periods. The proposed scheme is tested against a regular RTO/PE on a forced circulation evaporator and the Williams-Otto CSTR. The former case displays the effect of the proposed scheme in avoiding constraint violations, while the latter case shows the economic improvements that the proposed scheme can yield. Both case studies show a reduction in estimate variability with respect to the traditional PE approach, thus the proposed framework is attractive for the optimization of noisy process systems.

1. Introduction

The economic operation of systems is of paramount importance in the chemical and process industries, which are becoming increasingly market-driven and competitive. To this end, model-based economic optimization has been an active field within the process systems engineering community in recent years. Chiefly among these methods is Real-Time Optimization (RTO [1]), which has been deployed in a variety of applications: e.g., a laboratory-scale flotation column [2], a pilot-scale carbon capture system [3, 4], as well as a hydrogen production network [5]. RTO uses a steady-state process model as well as an economic model to determine the optimal operating point for the plant while addressing model uncertainty. These operating points are passed as set points to a control layer, which dynamically steers the plant towards the economic optimum.

While RTO typically employs detailed models that are a suitable reflection of the plant behaviour, often those models are subject to uncertainty, which can cause erroneous operating points that lead to economic suboptimality and constraint violations when implemented in the plant. Differences between the model and plant result in suboptimal plant economics as the model being optimized may not be fully equivalent with the plant it represents. The uncertainties present in RTO problems that cause these suboptimalities can be either structural (i.e., the model does not fully account for the phenomena occurring in the plant) or parametric (i.e., the model contains parameters that are not known precisely and/or may change over time) [6]. While structural model uncertainty in RTO is also an active research area [7, 8], parametric uncertainty is of interest in the present study.

To mitigate the effects of parametric uncertainty and arrive near the "true" economic optimum (i.e., the optimum that corresponds to the plant), a Parameter Estimation (PE) step is typically implemented alongside the economic optimization step in RTO via the so-called two-step approach. The PE step uses steady-state process information (i.e., historical data on the steady-state measurements and manipulated variables) to perform a least squares optimization problem, whereby the difference between measurements and the steady-state process model predictions are minimized with the uncertain parameters as the decision variables [9]. These updated parameters are subsequently supplied to the RTO problem and can be also supplied to the controller (e.g., in a model-based control scheme that uses a dynamic version of the RTO model). Once a new set point is achieved, the PE step is repeated as new steady-state data becomes available. Thus, the procedure of executing PE and RTO is performed periodically such that the plant and the model are constantly being reconciled through the model parameters. This overall scheme is closed loop since the RTO set points are passed to a regulatory controller, which acts on the plant, whereby plant measurements are supplied to the PE problem and the controller. Note that the associated problem of identifying whether steady state has been reached (known as steady state identification (SSI, [10])) is also a part of many RTO schemes. While SSI can be used to indicate when it is appropriate to begin collecting steady-state measurements, it does not otherwise interact with the PE and RTO in parameter estimation or set point generation, respectively; thus, its deployment is often omitted in the context of RTO for simplicity.

Issues arising from the use of experimental measurements often arise in practice, which could lead to performance loss in downstream operating layers. For instance, systematic measurement errors caused by instrumentation miscalibration or faults can occur and lead to poor estimation, monitoring, and control performance. To address this, gross error detection (GED) methods have been proposed in the literature, e.g., hypothesis testing [11], error bounds

[12], mixed integer programming [13], and maximum *a posteriori* estimation [14]. In the presence of faults, the deployment of GED in the context of PE/RTO will ensure that estimated parameters and set points are consistent with the plant thereby preventing erroneous operating points.

In addition to gross error, random error is also present and difficult to eliminate from industrial systems. This type of error occurs as measurements are subject to fluctuations obeying an underlying statistical distribution that causes imprecision [15]. In the context of RTO, variations in the set point produced by the RTO owed to noisy parameter estimates can occur [16]; these are caused by noisy plant measurements that lead to ill-conditioning in the PE problem and propagation of noise into the estimates. This set point imprecision is detrimental to the process economics as the effect of deviating from the true optimum may accrue substantially many RTO iterations. Moreover, fluctuating set points also impose undue burden on the process control layer, which is preferably avoided. To address the accuracy/precisions of RTO set points, a variety of approaches have been proposed in the literature.

A probability constrained approach has been proposed [17] to incorporate uncertain economics and constraints into a robust RTO formulation. However, robust approaches such as this sacrifice performance to find a solution that works well *regardless* of the true parameter realization. Other authors [18], have developed statistical approaches to decide when set point should be changed to avoid transients caused by insignificant parameter/disturbance changes. These use hypothesis testing and only perform model and set point updates upon the occurrence of significant changes in operating point; however, this does not address the root issue of noisy measurements and only avoids frequent unnecessary unwarranted set point fluctuations. Data reconciliation (DR), which makes experimental data consistent with the process model [11−15], can also be employed to improve two-step RTO performance such that the measurement and parameter estimates are consistent with the RTO model and constraints; this may have some noise-filtering effects, thus reducing variability. However, the main issue being addressed in DR is measurement/model consistency, not random error, and any effect that it has on random error may be an ancillary benefit. Increasingly, joint parameter and state estimation has been investigated along with the use of dynamic data to improve RTO performance by increasing execution frequency. A recent work [19] performed dynamic estimation whereby the set of estimated variables changed depending on the operating conditions; other contributions [20−22] have coupled dynamic parameter estimation with steady-state economic optimization to achieve increased RTO frequency. Nevertheless, the issue of noise propagation can persist in joint parameter and state estimation if not addressed. Lastly, robust estimators [11, 13, 15] have been proposed for GED, DR, and PE in chemical systems. These broadly aim to reduce the effects of outliers on parameter estimates by reformulation of the respective optimization problems (e.g., log-likelihood objectives); however, their effect on RTO has not been previously studied.

In general, the methods listed above require the implementation of new process layers [12, 19, 20] (e.g., Kalman filter or MHE) to generate outputs to the existing PE and RTO, thus further complicating an already stratified and intensive two-step approach. Other methods require sensitivity information [18, 19], which is difficult to estimate in practice as it requires system perturbations; this is particularly difficult in the presence of significant noise. The additional complexity proposed by these methods may be undesirable in an industrial setting as operators are reticent to implement convoluted operating schemes. Moreover, no method in the literature (i.e., [11−22]) aims to abate the effect

of random error explicitly in the context of RTO. This leaves a gap for a scheme that directly targets the effect of random error owed process noise in the two-layer RTO scheme.

To the authors' knowledge, a scheme to abate the effect of noise directly in parameter estimates in RTO has not been proposed in the literature. The present study introduces a low-variance PE (lv-PE) algorithm coupled with RTO for the economic operation of noisy processes. The lv-PE scheme reduces the error in parameter estimates with a twofold strategy. Firstly, the available measurements are probed for their information content to ensure low parameter variability (i.e., high precision) by performing "challenger" PE problems with different measurement combinations; this ensures that most of the information-rich measurements are used for PE. Secondly, a filter is introduced to reduce the frequency of high-error estimates by establishing parameter bounds; this prevents estimates beyond realistic bounds to be implemented in the system. Using the measurement-probing and data-filtering steps, the proposed method results in low measurement-to-parameter noise propagation and elimination of high-error estimates. The deployment of the proposed method does not entail a fundamental redesign of the two-layer RTO scheme that is prevalent in industry; this makes it an attractive way to augment RTO performance in any system that uses the two-layer approach. As will be shown in the following sections, the method only requires additional computations to be performed using the recurrently sampled measurements which would be collected nonetheless. Notably, this approach is not mutually exclusive with any aforementioned technique (i.e., GED, DR, robust estimation) since it chooses favourable measurements (pre-estimation) and filters noise from the resulting estimates (post-estimation). The proposed method can be used to improve the efficacy of robust estimators in noisy conditions and be included as an extra data-processing step with data reconciliation, gross error detection, or any online estimation task (e.g., state estimation).

The study is structured as follows: preliminary notation and standard definitions are defined at the outset; section 2 outlines the regular formulations for RTO, PE, and nonlinear model predictive control (NMPC) to expound on the arising issues with PE and provide context for the proposed algorithm. Section 3 presents, and rigorously motivates the proposed algorithm, also providing frameworks to analyze process economics and constraint violations in RTO-operated systems. Section 4 illustrates the implementation of the proposed algorithm through two case studies: an evaporator process and the Williams-Otto process. Section 5 summarizes the findings and provides areas of future work.

Preliminaries

Bolded letters denote matrices and vectors, while plain letter done scalars. Lower-case bolded letters denote vectors, while upper-case bolded letters denote matrices. $I_{n_i} \in \mathbb{R}^{n_i \times n_i}$ denotes an identity matrix of dimensions $n_i \times n_i$. $I_{n_i:j} \in \mathbb{R}^{n_i \times (n_i+1)}$ denotes a matrix composed of the identity matrix of dimensions $i \times i$ with a zero vector of length i inserted as column j, e.g.:

$$I_{3:3} = \begin{bmatrix} 1 & 0 & 0 & 0 \\ 0 & 1 & 0 & 0 \\ 0 & 0 & 0 & 1 \end{bmatrix} \tag{1}$$

Given a generic vector $x = [x_1 \quad \cdots \quad x_n]^T$, some operations on the vector are defined. $\|x\|_A^2$ denotes a quadratic form on the vector $x \in \mathbb{R}^{n_x}$ with the weighting matrix $A \in \mathbb{R}^{n_x \times n_x}$. $\hat{x} \in \mathbb{R}^{n_x}$ denotes model prediction of $x \in \mathbb{R}^{n_x}$. Model predictions are not inputs to the model nor the decision variables; rather, they are generated while solving

optimization problems but not conveyed to any other layers unless explicitly stated. $\{x_{t-i}\}_{i=0}^{N}$ denotes a discrete sequence of the vector x from the present time t to time $t - N$. $\bar{x} \in \mathbb{R}^{n_x}$ denotes the average of the sequence and σ_x denotes the standard deviation of that sequence, i.e.:

$$\bar{x} = \frac{1}{N} \sum_{i=-N}^{0} x_{t+i} \tag{2}$$

$$\sigma_x = \sqrt{\frac{\sum_{i=-N}^{0}(x_{t+i} - \bar{x})^2}{N-1}} \tag{3}$$

Similarly, the covariances of elements within the vector x given their discrete sequence $\{x_{t-i}\}_{i=0}^{N}$ is estimated as follows:

$$K_{i,j} = \frac{1}{N} \sum_{k=0}^{N}(x_{i,t-k} - \bar{x}_i)(x_{j,t-k} - \bar{x}_j) \quad \forall i \in \{1, \dots, n_x\}, \forall j \in \{1, \dots, n_x\} \tag{4}$$

The latter expression can be used to construct the covariance matrix $K_x \in \mathbb{R}^{n_x \times n_x}$. Lastly, this study uses $US\$$ as the monetary basis.

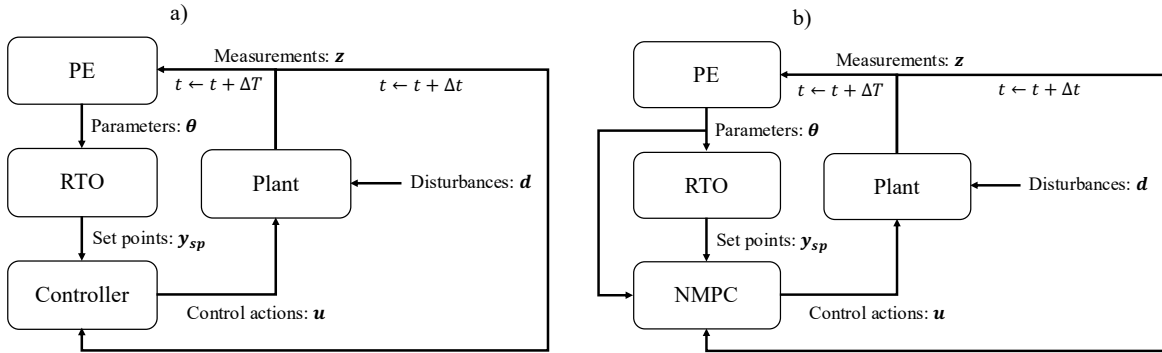## 2. Real-time optimization for controlled plants

Figure 1: Typical RTO scheme for a controlled plant with a) independent optimization and control models, b) equivalent optimization and control models.

Figure 1 depicts the exchange of information between the plant, RTO, PE, and controller via the two-step approach. Herein, a continuous plant is assumed to be subject to measurable disturbances ($d \in \mathbb{R}^{n_d}$). Note that this assumption is made for simplicity (i.e., measurability is not necessary for the proposed method as will be discussed later in this section). Measurements ($z \in \mathbb{R}^{n_z}$) can be acquired from the plant such that enough new data is collected to perform the PE problem at every RTO period ΔT. The PE problem supplies the RTO economic optimization problem with updated model parameters ($\theta \in \mathbb{R}^{n_\theta}$) which, in turn, supplies the controller with set points ($y_{sp} \in \mathbb{R}^{n_y}$). Note that y denotes the controlled variables that are regulated towards their respective set points (y_{sp}). The controller regulates the plant towards the RTO-supplied set points at every sampling interval Δt such that the plant is kept on target. Note that $\Delta T = k\Delta t$ where $k \in \mathbb{Z}^+$ (i.e., the RTO period is a positive integer multiple of the sampling interval), and typically $\Delta T \gg \Delta t$. Moreover, while state accessibility is often an issue in process plants (e.g., [4]), we assume that the required measurements are accessible for the purposes of this work (i.e., full state access is considered); this is not necessary for the scheme but done for simplicity and to remove confounding factors.

Two controller implementations are possible as depicted in Figure 1, a) when the controller uses an individual internal model/scheme and, b) when the RTO, PE, and controller models are equivalent (i.e., they use dynamic and steady state versions of the same model). The latter case is of primary interest as parameter updates are passed to both RTO and controller, thus affecting the scheme's performance in a twofold manner. For the purposes of this study, the parameter estimates are passed to both layers; however, they need only be passed to the RTO or NMPC layers to affect the system operation. Indeed, in larger systems where the online mechanistic control problem is expensive to compute, the use of a mechanistic MPC may be impractical such that the controller will be incompatible with PE. The use of equivalent models often necessitates that the controller uses detailed process models to match the PE and RTO layers, which are typically nonlinear, hence the use of nonlinear model predictive control (NMPC), as depicted in Figure 1b. The NMPCs employed herein use a dynamic version of the steady-state model deployed in the RTO and PE. Indeed, the interaction between NMPC and RTO has been studied previously [23, 24]; to the authors' knowledge, studies addressing a reduction of parameter variability owed to measurement noise are not available in the literature. Generally, RTO problems are formulated as follows:

$$
\begin{aligned}
&\min_{y} \Phi \\
&s.t. \\
&f_s(\hat{x}, y, u, d, \theta) = 0 \\
&g_s(\hat{x}, u, d) \leq 0 \\
&y^l \leq y \leq y^h \\
&u^l \leq u \leq u^h
\end{aligned}
\tag{5}
$$

where $\Phi \in \mathbb{R}$ denotes the economic model for which the process is optimized. In formulation (5), it is assumed that Φ is an economic loss function being minimized; however, maximization of a revenue function also occurs. The inputs to the RTO formulation (5) are the current process disturbances (d) and the uncertain model parameters (θ), while the outputs are the economically optimal controlled variables ($y \in \mathbb{R}^{n_y}$). The process state predictions ($\hat{x} \in \mathbb{R}^{n_x}$) and the manipulated variables ($u \in \mathbb{R}^{n_u}$) corresponding to the optimal set points are also generated by the model. $f_s: \mathbb{R}^{n_u} \times \mathbb{R}^{n_d} \times \mathbb{R}^{n_\theta} \longrightarrow \mathbb{R}^{n_x} \times \mathbb{R}^{n_y}$ denotes the steady-state process model. y^l and $y^h \in \mathbb{R}^{n_y}$ are lower and upper bounds for the set points, respectively, while u^l and $u^h \in \mathbb{R}^{n_u}$ are lower and upper bounds, respectively, for the manipulated variables. $g_s: \mathbb{R}^{n_x} \times \mathbb{R}^{n_u} \times \mathbb{R}^{n_d} \longrightarrow \mathbb{R}^{n_g}$ are any constraints (aside from those on the inputs and set points) to which the economic optimum must adhere. The RTO supplies the controlled variable set points to the controller (i.e., y_{sp}). Although the RTO may provide a set point that is challenging to match by the controller because of model uncertainty in both layers, the set point is nonetheless conveyed between the layers as it approximates the economic optimum (with some error); this point is described in the following section. Executing the RTO (and corresponding PE) problem too frequently would put undue computational burden on the plant and may not necessarily lead to drastic improvement in performance. Accordingly, the RTO problem is executed every RTO period ΔT as specified by the user, such that the set point is periodically being updated as more plant data becomes available. In contrast, the controller acts on the plant at every sampling interval Δt.

The controller is tasked with regulating the controlled variables towards the RTO-defined set points. In the case of an equivalent model between layers (Figure 1b) an NMPC can be considered. NMPC (or MPC more generally) takes plant state measurements or estimates at every sampling interval Δt and uses them as initial conditions for a process

model to predict plant behaviour on the horizon P. The manipulated variables are used as decision variables on the horizon C such that the NMPC generates the sequence $\left\{\boldsymbol{u}_{t+j}\right\}_{j=1}^{C}$ ($C \leq P$ such that $\boldsymbol{u}$ is assumed to remain constant beyond C). The first instance of manipulated variables from this sequence $\boldsymbol{u}_{t+1}$ are subsequently provided to the plant such that the system is controlled. The NMPC problem is formulated as follows:

$$\min_{\boldsymbol{u}_{t+j}\forall j\in\{1,...,C\}} \sum_{i=1}^{P}\left\|\boldsymbol{y}_{sp} - \widehat{\boldsymbol{y}}_{t+i}\right\|_Q^2 + \sum_{j=1}^{C}\left\|\Delta\boldsymbol{u}_{t+j}\right\|_R^2$$

$s.t.$

$$\boldsymbol{f}_d\left(\widehat{\boldsymbol{x}}_{t+i}, \widehat{\boldsymbol{y}}_{t+i}, \boldsymbol{u}_{t+j}, \boldsymbol{d}_{t+i}, \boldsymbol{\theta}\right) = \widehat{\boldsymbol{x}}_{t+i+1} \qquad \forall i \in \{1,...,P-1\}\, \forall j \in \{1,...,C\}$$
$$\boldsymbol{x}_t = \boldsymbol{x}_0$$
$$\boldsymbol{g}_d\left(\widehat{\boldsymbol{x}}_{t+i}, \boldsymbol{u}_{t+j}, \boldsymbol{d}_{t+i}\right) \leq \boldsymbol{0} \qquad \forall i \in \{1,...,P\}\, \forall j \in \{1,...,C\}$$
$$\boldsymbol{y}^l \leq \widehat{\boldsymbol{y}}_{t+i} \leq \boldsymbol{y}^h \qquad \forall i \in \{1,...,P\}$$
$$\boldsymbol{u}^l \leq \boldsymbol{u}_{t+j} \leq \boldsymbol{u}^h \qquad \forall j \in \{1,...,C\}$$

(6)

where all variables are defined as in the RTO with an additional dependence on time. The first term of the objective function represents a minimization of the sum of squared errors between the controlled variables and their set points over the horizon P, while the second term minimizes the squared changes in the manipulated variables from one time period to the next (i.e., $\Delta\boldsymbol{u}_{t+j+1} = \boldsymbol{u}_{t+j+1} - \boldsymbol{u}_{t+j}\,\forall j \in \{1,...,C\}$). These objective function terms affect control performance and manipulated variable speed, and are subject to the diagonal weighting matrices $\boldsymbol{Q} \in \mathbb{R}^{n_y \times n_y}$ and $\boldsymbol{R} \in \mathbb{R}^{n_u \times n_u}$, respectively, which are determined from prior tuning. $\boldsymbol{f}_d: \mathbb{R}^{n_u} \times \mathbb{R}^{n_d} \times \mathbb{R}^{n_\theta} \longrightarrow \mathbb{R}^{n_x} \times \mathbb{R}^{n_y}$ denotes the dynamic process model. $\boldsymbol{g}_d: \mathbb{R}^{n_x} \times \mathbb{R}^{n_u} \times \mathbb{R}^{n_d} \longrightarrow \mathbb{R}^{n_g}$ are the set of inequality constraints (aside from the controlled and manipulated variable constraints) that are imposed on the predicted trajectories. The inputs to the NMPC dynamic optimization problem are the initial conditions $\boldsymbol{x}_0 \in \mathbb{R}^{n_x}$, which are state measurements or estimates; as well as the disturbance trajectories ($\boldsymbol{d}_t = \cdots = \boldsymbol{d}_{t+P}$) and the model parameters ($\boldsymbol{\theta}$), which are assumed to remain constant at the latest disturbance and PE-defined value for the entire controller prediction horizon, respectively. The outputs of this problem are the optimal manipulated variable trajectory ($\boldsymbol{u}_{t+j} \in \mathbb{R}^{n_u}$) as well as the predicted state ($\widehat{\boldsymbol{x}}_{t+i} \in \mathbb{R}^{n_x}$) and controlled variable trajectories ($\widehat{\boldsymbol{y}}_{t+i} \in \mathbb{R}^{n_y}$). Only the first time-instance of the manipulated variables trajectory (i.e., $\boldsymbol{u}_{t+1}$) is implemented in the plant. After this, the plant is operated for a sampling interval Δt whereby new measurements are given to the NMPC as feedback and the formulation in equation (6) is re-solved; therefore, the process of sampling and solving the NMPC problem is repeated recursively, and the scheme becomes closed-loop.

The uncertain model parameters ($\boldsymbol{\theta}$) associated with formulations (5) and (6) must be estimated prior to every execution of the RTO problem (5) to reconcile the plant model with the current steady state operating conditions. The PE optimization problem is based on Bayesian inference, which allows for the embedding of prior information and determination of weighting terms in a statistically rigorous manner. This assumes that measurements (and thus the noise associated with measurements) obey a Gaussian distribution; the complete outline of the probabilistic interpretation can be found elsewhere [9]. As such, the work herein is limited to Gaussian noise, which is indeed a very common assumption in process systems.

The PE problem uses a measurement sequence $\{z_{t-i}\}_{i=0}^{M}$, whereby the past M steady-state samples are considered. This allows for averaged measurements ($\bar{z} \in \mathbb{R}^{n_z}$) to be computed using equation (2) along with the measurement covariance matrix ($K \in \mathbb{R}^{n_z \times n_z}$) using equation (4). The PE problem is as follows:

$$\min_{\theta} \|\hat{z} - \bar{z}\|_{K^{-1}}^{2}$$
$$s.t.$$
$$f_s(\hat{x}, \hat{y}, \bar{u}, \bar{d}, \theta) = 0$$
$$h_s(\hat{x}, \bar{u}, \bar{d}) = \hat{z} \tag{7}$$
$$g_s(\hat{x}, \bar{u}, \bar{d}) \leq 0$$
$$\theta^l \leq \theta \leq \theta^h$$

$f_s: \mathbb{R}^{n_u} \times \mathbb{R}^{n_d} \times \mathbb{R}^{n_\theta} \longrightarrow \mathbb{R}^{n_x} \times \mathbb{R}^{n_y}$ is the steady-state process model that also corresponds to the model used in formulation (5). θ^l and $\theta^h \in \mathbb{R}^{n_\theta}$ are lower and upper bounds, respectively, for the parameter estimates. $g_s: \mathbb{R}^{n_x} \times \mathbb{R}^{n_u} \times \mathbb{R}^{n_d} \longrightarrow \mathbb{R}^{n_g}$ are any constraints (aside from those on the inputs and set points) to which the estimates must adhere. Moreover, $h_s: \mathbb{R}^{n_x} \times \mathbb{R}^{n_u} \times \mathbb{R}^{n_d} \longrightarrow \mathbb{R}^{n_z}$ denotes the function between the model inputs and measurement prediction. The measurements can coincide with the states or be functions of the model inputs/states. The objective function in problem (7) minimizes the differences between the model measurement predictions and the sample-averaged measurements by using the model parameters as the decision variables. The inverse covariance matrix (K^{-1}) weights the objective function such that high-variance measurements are assigned low weights with the converse occurring for low-variance measurements. By performing the sampling and averaging, less noisy reconciliation between plant and model are achieved; however, some noise will still propagate to the parameter estimates as experimental data are used. In executing this formulation, the plant and model are reconciled for current operating conditions as the latest available steady-state plant data including the measurements, manipulated variables, and disturbances are used. As such, the inputs to this problem are the averaged measurements ($\bar{z}$), averaged manipulated variables ($\bar{u}$), and disturbances ($\bar{d}$) while the outputs are the parameter estimates (θ). While a large M would be preferable for its averaging effect (especially in the presence of noise), this can lead to the use of measurements that are not truly at steady state (e.g., owing to drift or subtle control actions over time); thus, the size of M is typically limited. Note that this formulation can also be adapted for disturbance estimation or joint parameter/disturbance estimation; however, this work is restricted to cases involving parameter estimation.

As both RTO and NMPC layers are privy to the parameter estimates, poor PE performance can lead to suboptimal operation via inaccurate RTO set points and set point offset in the NMPC layer when compared to the true optimum. Given the formulations presented above, the importance of the PE problem becomes clear from the dependence of the RTO and NMPC on θ. Moreover, the gaps for a method to deal with variation in parameter estimates can be expounded upon:

1) More information (i.e., measurements) do not necessarily mean that the PE problem (7) will yield better estimates as covariances (K) may, in fact, weigh the problem unevenly such that it becomes ill-conditioned. Typically, all available measurements (z) are used when solving PE problems; accordingly, there is need for a method that can choose a favourable subset of measurements to provide to the PE step.

2) Problem (7) uses a sample of measurements ($\{z_{t-i}\}_{i=0}^M$), which are subject to noise through the sample average $\bar{z}$ and the covariance matrix K. The propagation of noise from the measurements to the parameter estimates can cause economic losses, which accrue in the long-term. There remains a gap for a method to ensure this does not occur by filtering for erroneous estimates.

To address these issues, the low-variance PE procedure is introduced herein and presented in the following section. This comprises an algorithm that determines favourable measurements to embed in the PE problem as well as a filter to reject instances where the parameters are poorly estimated.

3. Low-variance parameter estimation (lv-PE)

The proposed low-variance PE (i.e., lv-PE) scheme works by reducing the variability in parameter estimates with respect to their expected value, which is equivalent to their true value provided that the system is absent of systematic errors (see assumption 3 below). Accordingly, any single estimate may not be more accurate at a given PE/RTO iteration; however, the estimates over time will be more precise, thus benefits will accrue over many RTO periods. In this section, the scheme is motivated through analysis of the set point error, which is attributed to parameter error. Then, the algorithm comprising the scheme is discussed step-by-step. Moreover, the economic implications of the method are discussed, with a novel algebraic and geometric interpretation of RTO economics. Assessment metrics for the scheme are introduced at the end of this section.

The following assumptions are made herein:

1) The time operating at steady state far exceeds the time operating dynamically. This is an underlying assumption in systems that operate with RTO [1] (i.e., not specific to the proposed approach) as the principle of steady-state optimization is that cost-optimal operating policy is steady while dynamic operation is expensive and should be minimized.

2) The measurement noise is additive Gaussian and occurs owing to random errors. As noted earlier, this is an underlying assumption of standard PE in equation (7) as the least-squares objective embedded with prior measurements arises from Bayesian inference in the presence of Gaussian noise [9].

3) Plant–model mismatch is owed to PE error. This is a standard assumption in the two-layer RTO [1] whereby a mechanistic model is assumed to provide an adequate representation of the system and only requires parameter estimates to match the plant. Mechanistic process models are increasingly common and available for RTO; however, in cases where such model is not available, other approaches [7,8] can be considered. The PE error herein is owed to large noises to which the measurements are subjected. Measurement bias and similar systematic errors are not addressed herein as they would require GED. In principle, GED could also be addressed within the proposed scheme but would require an extra processing layer as indicated in the introduction. However, as this is the first study to use the proposed approach, extra layers were not considered to explicitly assess the benefits and limitations of the method.

3.1. Effect of parameters error on set point tracking

A theoretical argument is first made to motivate the proposed approach, which connects parameter error to set point error for an RTO-operated system. Consider a single RTO period during which the process loss is minimized (alternatively, revenue can be maximized). For a constrained RTO to operate the process at its "true" economic

optimum (i.e., the economic optimum corresponding to the plant, not the mismatched model) the controlled variables must fulfill the Karush-Kuhn-Tucker (KKT) conditions, i.e.:

$$\nabla\Phi\left(y_{sp}^{true}\right) + J_f\left(y_{sp}^{true}\right)^T \lambda + J_g\left(y_{sp}^{true}\right)^T \mu = 0$$
$$f\left(y_{sp}^{true}\right) = 0$$
$$g\left(y_{sp}^{true}\right) = 0 \tag{8}$$
$$\mu^T g\left(y_{sp}^{true}\right) = 0; \mu \geq 0$$

where $J_f \in \mathbb{R}^{n_x \times n_y}$ and $\lambda \in \mathbb{R}^{n_x}$ are the Jacobian matrix and KKT multipliers of the process model, respectively. Moreover $J_g \in \mathbb{R}^{n_g \times n_y}$ and $\lambda \in \mathbb{R}^{n_g}$ are the Jacobian matrix and KKT multipliers of the process constraints, respectively. $y_{sp}^{true} \in \mathbb{R}^{n_y}$ in equation (8) denotes the controlled variables set points that achieve a true economic optimum (i.e., plant KKT conditions). In practice, the true economic optimum y_{sp}^{true} is difficult to achieve because of mismatch between the plant and RTO model. As such, the performance of an RTO optimizer can be assessed by the difference between the actual controlled variables achieved by the system and the true set points. Over time, this can be quantified using an error metric; herein the integral square error (ISE) is considered owed to its common use in control systems. Accordingly, the error is quantified over the single RTO operating period ($T_{RTO} = \Delta T$):

$$ISE = \int_0^{T_{RTO}} \left\| y^{RTO} - y_{sp}^{true} \right\|_{I_{n_y}}^2 dt \tag{9}$$

where $y^{RTO} \in \mathbb{R}^{n_y}$ denotes the actual controlled variables achieved by the RTO-operated system. y_{sp}^{true} and y^{RTO} are distinct as the RTO may not operate the system at the theoretical optimum owing to modelling errors, thus the gap between the achieved set point and the true optimum is expressed by the error metric in equation (9). The set point offsets in equation (9) provide a way to analyze the efficacy of an RTO-operated system on a theoretical basis. As values of y^{RTO} are not known a priori, the effect of offset is analyzed under several hypothetical scenarios as shown next.

The operation of process plants is composed of many RTO periods; however, taking a more granular view as done here, a single RTO operating period can be segmented into distinct phases: the suboptimal phase, the dynamic phase, and the optimal phase; these are depicted in Figure 2. The suboptimal phase corresponds to the time before the RTO is executed and the system is operating at a point that is outdated/suboptimal ($y^{sub} \in \mathbb{R}^{n_y}$), the dynamic phase occurs once the RTO has been executed and the system is in a transient state ($y^{dyn} \in \mathbb{R}^{n_y}$), and the optimal phase occurs once the system is operating at its RTO-defined set point ($y^{opt} \in \mathbb{R}^{n_y}$). Note that the "optimal phase" here corresponding to y^{opt} refers to optimal as achieved by the PE/RTO-operated system and may, in fact, not be the true plant optimum y_{sp}^{true} as the RTO can result in offset with respect to the true set point as show in equation (9). The segmentation of the RTO period into three phases allows for y^{RTO} as defined previously to be decomposed into y^{sub}, y^{dyn}, and y^{opt}. These phases have durations t_{sub}, t_{dyn}, and t_{opt}, such that for a single RTO period $T_{RTO} = t_{sub} + t_{dyn} + t_{opt}$.
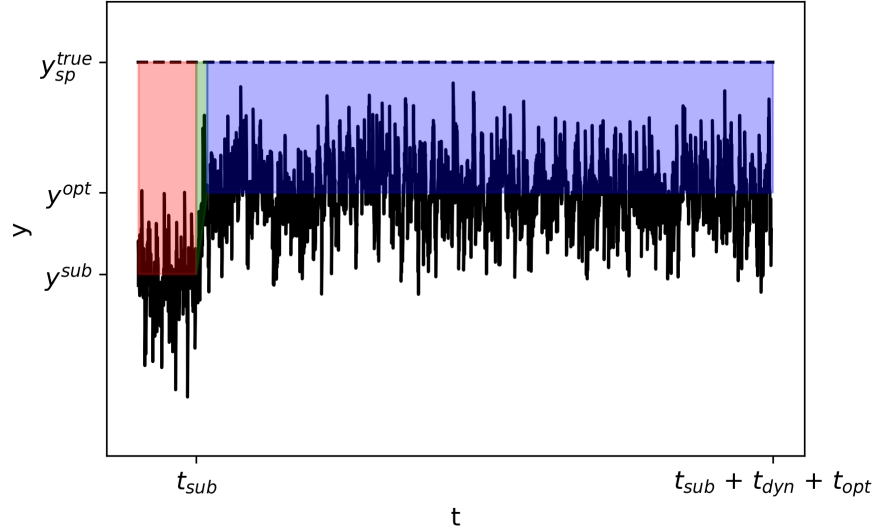
Figure 2: Segmentation of RTO period. Dotted (--) line denotes the true (theoretical) optimum. The integral of differences between true optimum and actual phase values highlighted red (suboptimal phase), green (dynamic phase), and blue (optimal phase).

This allows for equation (9) to be segmented into phases, for which the set point difference in each phase is shown in Figure 2 as follows:

$$ISE = \int_0^{t_{sub}} \left\| y^{sub} - y^{true}_{sp} \right\|^2_{I_{n_y}} dt + \int_{t_{sub}}^{t_{dyn}+t_{sub}} \left\| y^{dyn} - y^{true}_{sp} \right\|^2_{I_{n_y}} dt + \int_{t_{sub}+t_{dyn}}^{t_{sub}+t_{dyn}+t_{opt}} \left\| y^{opt} - y^{true}_{sp} \right\|^2_{I_{n_y}} dt \quad (10)$$

Since RTO is inherently a steady state method, assumption 1 outlined above is made; indeed, predominantly steady state operation is largely the case for many process plants. This leads to $t_{sub}, t_{opt} \gg t_{dyn} \implies T_{RTO} \cong t_{sub} + t_{opt}$, thus simplifying equation (10) to:

$$ISE = \int_0^{t_{sub}} \left\| y^{sub} - y^{true}_{sp} \right\|^2_{I_{n_y}} dt + \int_{t_{sub}}^{t_{sub}+t_{opt}} \left\| y^{opt} - y^{true}_{sp} \right\|^2_{I_{n_y}} dt \quad (11)$$

The RTO-defined controlled variables can be partitioned into the true value (as defined above) and their deviation from the true value ($\sigma \in \mathbb{R}^{n_y}$), which allows for the expansion into:

$$ISE = \int_0^{t_{sub}} \left\| y^{true}_{sp} + \sigma^{sub} - y^{true}_{sp} \right\|^2_{I_{n_y}} dt + \int_{t_{sub}}^{t_{sub}+t_{opt}} \left\| y^{true}_{sp} + \sigma^{opt} - y^{true}_{sp} \right\|^2_{I_{n_y}} dt \quad (12)$$

which simplifies to:

$$ISE = \int_0^{t_{sub}} \left\| \sigma^{sub} \right\|^2_{I_{n_y}} dt + \int_{t_{sub}}^{t_{sub}+t_{opt}} \left\| \sigma^{opt} \right\|^2_{I_{n_y}} dt \quad (13)$$

Moreover, as only steady state periods are being analyzed, the deviations from the true values are constant for a single given RTO period (i.e., not a function of time) as show geometrically in Figure 2. The solution of equation (13) provides a definition of the *ISE* performance metric for RTO:

11

$$ISE = \left\|\boldsymbol{\sigma}^{sub}\right\|_{I_{n_y}}^{2} t_{sub} + \left\|\boldsymbol{\sigma}^{opt}\right\|_{I_{n_y}}^{2} t_{opt} \tag{14}$$

Using equation (14), the performance of two operating schemes can be compared: the first (lv), which reduces the set point deviation; and the second (r), which is the regular RTO problem:

$$ISE_{lv} - ISE_{r} = \left\|\boldsymbol{\sigma}_{lv}^{sub}\right\|_{I_{n_y}}^{2} t_{sub,lv} + \left\|\boldsymbol{\sigma}_{lv}^{opt}\right\|_{I_{n_y}}^{2} t_{opt,lv} - \left\|\boldsymbol{\sigma}_{r}^{sub}\right\|_{I_{n_y}}^{2} t_{sub,r} - \left\|\boldsymbol{\sigma}_{r}^{opt}\right\|_{I_{n_y}}^{2} t_{opt,r} \tag{15}$$

To have an equivalent assessment of the schemes, it can be assumed that both operating schemes in equation (15) begin at the same suboptimum (i.e., $\boldsymbol{\sigma}_{lv}^{sub} = \boldsymbol{\sigma}_{r}^{sub}$) and can act at the same time (i.e., $t_{sub,lv} = t_{sub,r} = t_{sub}$ and $t_{opt,lv} = t_{opt,r} = t_{opt,}$), thus:

$$ISE_{lv} - ISE_{r} = \left(\left\|\boldsymbol{\sigma}_{lv}^{opt}\right\|_{I_{n_y}}^{2} - \left\|\boldsymbol{\sigma}_{r}^{opt}\right\|_{I_{n_y}}^{2} \right) t_{opt} \tag{16}$$

Which, since $t_{opt} > 0$ by definition, leads to:

$$ISE_{lv} - ISE_{r} < 0 \Longleftrightarrow \left\|\boldsymbol{\sigma}_{lv}^{opt}\right\|_{I_{n_y}}^{2} < \left\|\boldsymbol{\sigma}_{r}^{opt}\right\|_{I_{n_y}}^{2} \tag{17}$$

Following assumption 3, it can be concluded that by reducing the error in parameter estimates ($\boldsymbol{\theta}$), the deviations from the set points are also minimized as the uncertain parameters represent the only source of plant–model mismatch, thus:

$$ISE_{lv} - ISE_{r} < 0 \Longleftrightarrow \left\|\boldsymbol{\sigma}_{\theta,lv}^{opt}\right\|_{I_{n_y}}^{2} < \left\|\boldsymbol{\sigma}_{\theta,r}^{opt}\right\|_{I_{n_y}}^{2} \tag{18}$$

Since the set point corresponding to $\boldsymbol{y}_{sp}^{true}$ is indeed an economic optimum by definition, the minimization of parameter deviations will lead to improved economics as effected through the set points. This can be generalized to multiple RTO periods if the deviations $\boldsymbol{\sigma}$ are re-defined as standard deviations, thus they represent the mean deviation across many RTO periods. An algorithm to achieve this lowering of parameter deviation, which fulfills the assumptions made herein is presented next.
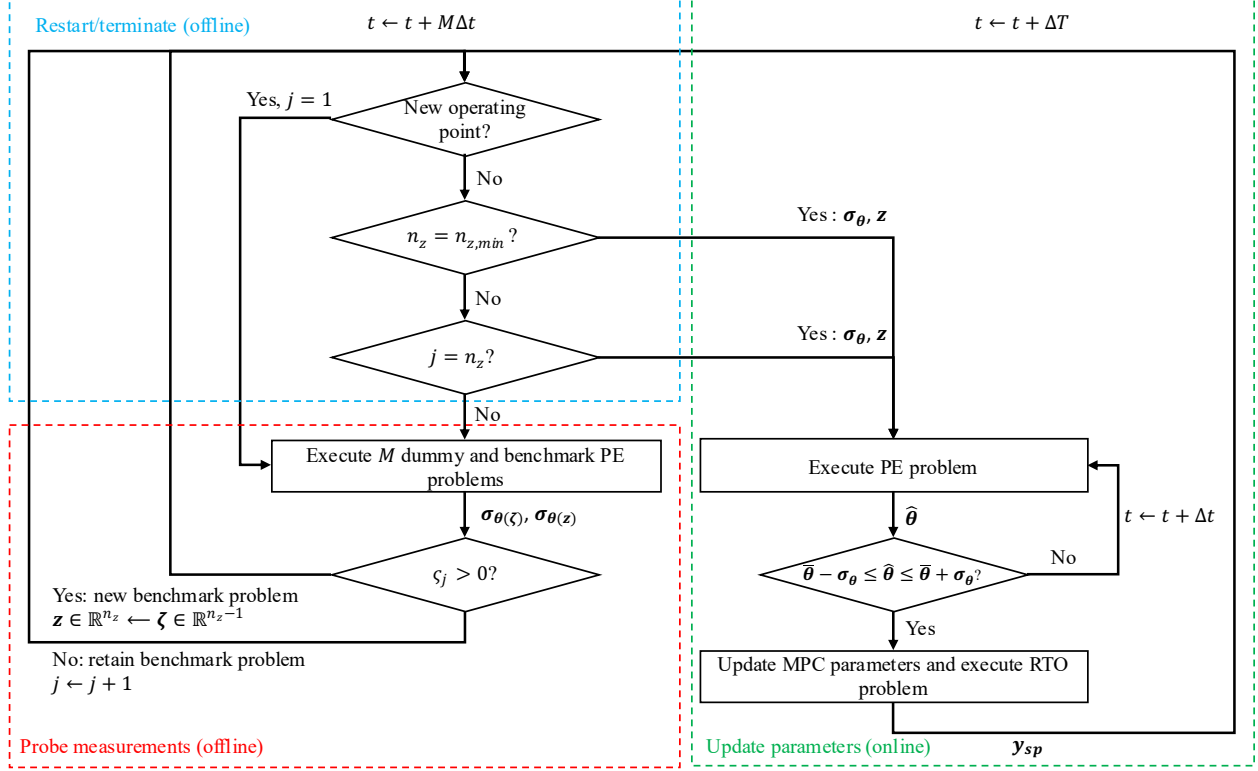
3.2. Proposed approach (lv-PE)

Figure 3: The proposed low-variation parameter estimation algorithm for RTO. The blue block denotes the restarting criteria for the measurement-probing block (in the red block). The green block denotes the parameter update procedure in the RTO and NMPC.

The proposed algorithm to lower the variability in the parameter estimates is depicted in Figure 3 and divided into three blocks to facilitate discussion. The key idea is to test available measurements sequentially for whether they help or hinder the variability of the parameter estimates by performing "challenger" PE problems (i.e., potential PE formulations of which the results are not implemented in the RTO or NMPC). The parameter estimates of the challenger problems are compared to those of a benchmark problem, whereby the challenger problem is a version of the benchmark problem with an omitted measurement. If the challenger problem performs better with the omitted measurement, it becomes the new benchmark problem. At the first iteration of the algorithm, the benchmark problem contains all available measurements, this way they may all be probed as the algorithm progresses; as the progression occurs, each successive benchmark problem will have a lower parameter variability. The removal of measurements is preferable to the addition of measurements as addition will require an initial subset of fixed measurements to be chosen *a priori*. Both challenger and benchmark problems are executed several times; accordingly, data regarding the parameter estimates is collected to calculate their statistical parameters. These are used twofold: 1) to determine the combination of measurements that leads to the lowest σ_θ^{opt}; 2) as filters to discard inaccurate parameter estimates (i.e., those outside of the tightest $\pm\sigma_\theta^{opt}$).

The scheme can begin at any point in the operation of a process by going through the restart/terminate block in Figure 3 (i.e., checking if an operating point change has occurred and if all conditions for the measurement-probing procedure are met). Once these conditions are met, the measurement-probing block in Figure 3 is activated (the activation conditions will be explained in detail at the end of this section). Upon activation, a counter is set to $j = 1$ and all

measurements are assumed to be used (i.e., $\mathbf{z_0} \in \mathbb{R}^{n_{z_0}}$ where $n_z = n_{z_0}$). The challenger problems as shown in the measurement-probing block of Figure 3 and defined in formulation (19) are solved M times over M sampling intervals Δt such that each problem has a data window with a new measurement added and an old measurement discarded with respect to the previous problem. This process of executing M challenger problems is performed by excluding a measurement from the benchmark PE problem via the formulation in equation (19). The challenger problems are performed offline such that their estimates are never conveyed to the other layers. At $j = 1$, the benchmark is the regular PE problem as defined in equation (7) with $\mathbf{z_0}$, and it is also solved M times over M sampling intervals. This benchmark problem will change if a better formulation is found by the challenger problem, otherwise is it kept.

The challenger PE problems are formulated as a modified PE problem where the variables are defined as in equation (7) except for $\boldsymbol{\zeta} \in \mathbb{R}^{n_z - 1}$. The challenger problems are as follows:

$$\min_{\boldsymbol{\theta}} \left\| \hat{\boldsymbol{\zeta}} - \bar{\boldsymbol{\zeta}} \right\|_{\kappa^{-1}}^2$$
$$s.t.$$
$$f_s\left(\hat{x}, \hat{y}, \bar{u}, \bar{d}, \boldsymbol{\theta}\right) = 0$$
$$h_s\left(\hat{x}, \bar{u}, \bar{d}\right) = \hat{z}$$
$$I_{n_z - 1 : j}\hat{z} = \hat{\boldsymbol{\zeta}} \qquad (19)$$
$$g_s\left(\bar{u}, \bar{d}, \hat{x}\right) \leq 0$$
$$\boldsymbol{\theta}^l \leq \boldsymbol{\theta} \leq \boldsymbol{\theta}^h$$

where $\hat{\boldsymbol{\zeta}}$ excludes measurement j from the PE problem using $I_{n_z - 1 : j} \in \mathbb{R}^{(n_z - 1) \times n_z}$ such that only a subset of measurements $\boldsymbol{\zeta}$ are used with the respective covariance matrix $\boldsymbol{\kappa} \in \mathbb{R}^{(n_z - 1) \times (n_z - 1)}$ and averages $\bar{\boldsymbol{\zeta}} = I_{n_z - 1 : j}\, \bar{z}$.

After M executions of problem (19), the parameter sequence $\left\{\boldsymbol{\theta}(\boldsymbol{\zeta})_{,t-i}\right\}_{i=0}^M$ is available, allowing for the calculation of the standard deviation of that sequence $\boldsymbol{\sigma}_{\boldsymbol{\theta}(\boldsymbol{\zeta})}$. Moreover, M executions of a benchmark PE problem (i.e., with the full set of measurements $\mathbf{z}$) have also been performed to obtain the sequence $\{\boldsymbol{\theta}(\mathbf{z})_{\,t-i}\}_{i=0}^M$ with variation benchmark $\boldsymbol{\sigma}_{\boldsymbol{\theta}(\mathbf{z})}$. Note that M is a system parameter and is limited by the RTO period size as it will determine the computational time associated with the proposed scheme along with the number of challenger problems required; more details about this parameter are provided in the following section.

The information content ($IC \in \mathbb{R}$) metric introduced by Vrugt, Bouten and Weerts [25] is adapted for PE as follows:

$$IC_{i,k} = 1 - \frac{\sigma_{\theta(\zeta),i,k}}{\sigma_{\theta(z),i,k}} \quad \forall i \in \{1, \dots, n_\theta\} \qquad (20)$$

where $k = j + n_{z_0} - n_z$ denotes the number of measurements probed hitherto.

The IC metric in equation (20) quantifies if, and by how much, the exclusion of a measurement helps in the decrease of parameter variability. $IC_{i,k} > 0$ implies that the removal of a measurement helps reduce variability while $IC_{i,k} < 0$ implies that the removal increases the variation. The IC metric was chosen due to its simplicity and the fact that it does not require plant perturbations such as alternatives metrics like the sensitivity matrix [26]. In essence, equation (20) determines whether each measurement is beneficial or detrimental to the expected error of the PE problem via parameter standard deviations. The deviations are used in evaluating a benchmark problem (i.e., with lowest variance set of measurements found thus far in the measurement probing phase) and a challenger problem (i.e., with a

potentially better set of measurements). To quantify the aggregate effect of measurement exclusion in systems with many parameters, the overall IC ($\varsigma_k \in \mathbb{R}$) is defined as follows:

$$\varsigma_k = \sum_{i=1}^{n_\theta} IC_{i,k} \tag{21}$$

This is depicted within the measurement-probing block of Figure 3 to determine whether to exclude or keep a measurement as follows:

If $\varsigma_k > 0$, the exclusion of the measurement is deemed beneficial as cumulative impact of the exclusion is net positive across all estimated parameters in the system (i.e., the variation in some parameters may decrease while the variance in other may increase; however, the net effect is of decrease in variation). As such, the measurement j being tested is removed from the PE formulation and the challenger formulation becomes the new benchmark problem, thereby reducing the dimension of the measurements vector by one i.e.,

$$n_z \leftarrow n_z - 1 \Longrightarrow \mathbf{z} \in \mathbb{R}^{n_z} \leftarrow \boldsymbol{\zeta} \in \mathbb{R}^{n_z - 1}$$

following this, the probing process then proceeds whereby the previous second measurement, which is now the first measurement (i.e., $z_1 \leftarrow z_2$), is probed for its information content.

If $\varsigma \leq 0$, the exclusion of the measurement is not beneficial, thus the measurement is retained, and a new exclusion candidate is chosen i.e., $j \leftarrow j + 1$.

This process is then repeated sequentially for available measurements $k \in \{1, \dots, n_{z_0}\}$ until either of the three conditions in the restart/terminate block of Figure 3 is fulfilled: 1) the operating point changes as dictated by a sudden disturbance to the system, thus interrupting the measurement-probing process and setting $j = 1$, 2) the minimum number of allowable measurements are reached as specified by the user based on identifiability analysis [27] or process knowledge or, 3) the scheme has gone through all the available measurements and chosen only to exclude a small subset. The latter two conditions are reflected in the following:

$$n_z = n_{z,min} \tag{22}$$

$$n_z = j \tag{23}$$

where $n_{z,min}$ is the minimum number of measurements required for the system to be identifiable. Condition (22) ensures that the minimum number of measurements needed (conversely, the maximum number of measurements that can be excluded) are retained. Additionally, condition (23) stops the data acquisition when all original measurements have been analyzed as reflected by the index k being equivalent to the original number of measurements n_{z_0} (and condition (22) has not yet been fulfilled). Condition (22) is predominant as reflected in Figure 3, whereby it is checked before condition (23); this is to ensure sufficient measurements always remain such that the system is identifiable.

Once the measurement-probing block of the algorithm in Figure 3 is completed, the information-rich measurement vector $\mathbf{z}$ is known and the filter bounds $[\overline{\boldsymbol{\theta}} - \boldsymbol{\sigma}_{\theta(z)}, \overline{\boldsymbol{\theta}} + \boldsymbol{\sigma}_{\theta(z)}]$ can be calculated using the parameter sample $\{\boldsymbol{\theta}(\mathbf{z})_{t-i}\}_{i=0}^{M}$ from the final benchmark problem (i.e., the one corresponding to the subset of measurements that were

chosen to be used in the PE problem implemented in the RTO and NMPC). The sample of parameter estimates corresponding to the chosen subset of measurements is used to calculate these bounds as the standard deviation. Since the standard deviation is the average difference between the expected parameter value and the individual estimates within the sample, future estimates outside of the bounds established by the standard deviation (i.e., those with higher-than-average distance from the expected parameter) are deemed unacceptable. This avoids potential high-error estimates whereby noisiness may be propagating excessively to the estimates. With this information, the PE problem (7) can be performed and implemented at every RTO period ΔT with the chosen subset of measurements $\mathbf{z}$ as depicted in the update block of Figure 3. This PE problem corresponds to the one with the final $\mathbf{z}$ determined by the measurement-probing block of the algorithm and generates the estimates $\widehat{\boldsymbol{\theta}}$, which are assessed with the filter bounds. If the estimates are outside the filter bounds, they are not accepted, and another sampling interval is taken to collect measurements; this process is repeated until an acceptable set of parameter estimates are generated. If the estimates are inside the filter bounds, the parameters are used to update the NMPC and execute the RTO problem.

The update procedure is not repeated for another RTO period (i.e., $t \leftarrow t + \Delta T$) unless a new operating point is introduced as depicted by the upper decision block in Figure 3, which restarts the measurement-probing process. When a sudden operating point change occurs, as indicated by a sudden large change in control actions or process economics, the measurement-probing block of the algorithm in Figure 3 is reactivated by the restart /terminate block. This is done to ensure that favourable measurements are being used for the PE problem under the new operating conditions. Note that 'favourable' measurements may not mean optimal as stopping criteria (22) may halt the algorithm before all measurements are probed for IC. Nevertheless, the subset of 'favourable' measurements chosen by the proposed scheme will always lead to parameter estimates that are equally accurate or more accurate than the original set of measurements. Alternatively, the measurement-probing block can also be activated through the restart/terminate block if there is a sudden change occurs as the measurement probing procedure is proceeding, this is checked for after every new challenger problem is introduced (i.e., $t \leftarrow t + M\Delt$).

In summary, the algorithm proceeds as follows:

lv-PE algorithm applied to RTO:	
1.	New operating point?
a.	Yes: activate measurement-probing block, go to step 4
b.	No: go to step 2
2.	$n_z = n_{z,min}$?
a.	Yes: activate parameter update block, go to step 5
b.	No: go to step 3
3.	$n_z = j$?
a.	Yes: activate parameter update block, go to step 5
b.	No: activate measurement-probing block, go to step 4
4.	Measurement-probing, set $j = 1$
a.	Execute M challenger and benchmark problems (19) and (7), respectively

i.	If $\varsigma_k > 0$: $j = 1$, measurement excluded, new benchmark problem established, go to step 1	
ii.	Else: $j += 1$, measurement retained, keep old benchmark problem, go to step 1	
5.	Parameter update	
a.	Execute actual PE problem	
i.	If $\overline{\boldsymbol{\theta}} - \boldsymbol{\sigma_\theta} \leq \widehat{\boldsymbol{\theta}} \leq \overline{\boldsymbol{\theta}} + \boldsymbol{\sigma_\theta}$: update RTO and MPC parameters, $t += \Delta T$, return to step 1	
ii.	Else: $t += \Delta t$, return to step 5a	

It should be noted that the algorithm presented above is designed to reduce parameter variation across RTO periods, not to detect gross errors. However, the method could be adjusted for GED through hypothesis testing [11] of the parameter estimate means generated by the benchmark and challenger problems in the lv estimation algorithm. Accordingly, a test statistic could be used to determine whether measurement removal in the probing procedure generates shifting means, thus identifying gross errors. The lv-PE, as proposed herein, has two major advantages over the regular PE applied to RTO: firstly, the most information-rich subset of measurements is chosen to reduce parameter variability; secondly, the parameter filter avoids RTO periods with poorly estimated parameters. As shown in the previous section, this will result in lower set point error and, in turn, better process economics. Importantly, the information content procedure only requires sampling and can be performed offline as its solutions are not implemented in the system being operated. The only time at which the proposed scheme interacts with the process control loop is when the RTO set points are updated. Otherwise, only an additional independent computer/processor is necessary for repeated execution of the PE problems, which do not interfere with the regular process control loop; this makes the requirements for implementation relatively simple, hence its appeal of industrial systems. The information content procedure may be adjusted through sample sizes such that it can fully occurs within the RTO period; the assessment of this computational expense to the PE computer will be elaborated on in the following section.

3.3. Scheme assessment and economic analysis

The proposed scheme is mainly analyzed through variation, the process economics, and constraint violations; these are the factors that affect the PE, NMPC, and RTO problems, which the scheme aims to improve upon. The variation is captured through the standard deviation of parameters, the economics are calculated using the process revenues/losses and their rates, and the constraint violations can be quantified through their cumulative magnitude.

As shown in section 3.1., the *ISE* of the operation of an RTO system is linearly dependent on the operating time; thus, the cumulative error can be written as a linear combination of the error terms of each individual RTO period. The same follows for the process economics $R(\$)$, where a revenue is made if $R > 0$ or a loss is incurred if $R < 0$. This occurs as the operation is a combination of constant rates $P(\$/time)$. $P > 0$ is a profit rate and occurs when the operator is selling produced commodities; in contrast $P < 0$ is a price rate and occurs when a process is operating at a loss.

As stated previously, the RTO period consists of three phases ($T_{RTO} = t_{sub} + t_{dyn} + t_{opt}$). These correspond to suboptimal operation before the set points are updated t_{sub} ($time$), a fast (i.e., negligible) dynamic operation, and RTO-optimal operation once the set points are updated t_{opt} ($time$). The respective suboptimal, dynamic, and optimal

process profit/cost rates are $P_{sub,i}$, $P_{dyn,i}$, and $P_{opt,i}$ ($/time$) are dependent on the specific RTO period i. This enables calculation of the cumulative process economics (i.e., as the process progresses), i.e.,

$$R = \sum_{i=0}^{N} \int_{0}^{T_{RTO}} P_i \, dt \tag{24}$$

Again, this can be segmented into three phases: suboptimal, dynamic, and optimal, i.e.:

$$R = \sum_{i=0}^{N} \int_{0}^{t_{sub}} P_{sub,i} \, dt + \int_{t_{sub}}^{t_{sub}+t_{dyn}} P_{dyn,i} \, dt + \int_{t_{sub}+t_{dyn}}^{t_{sub}+t_{dyn}+t_{opt}} P_{opt,i} \, dt \tag{25}$$

As the RTO operation is inherently steady state, the dynamics are assumed to ensure quickly, thus simplifying to:

$$R = \sum_{i=0}^{N} \int_{0}^{t_{sub}} P_{sub,i} \, dt + \int_{t_{sub}}^{t_{sub}+t_{opt}} P_{opt,i} \, dt \tag{26}$$

Both suboptimal and optimal phases are composed of constant profit/loss rates whereby the time that is not spent operating optimally during the RTO period is spent operating suboptimally instead, this can be expressed as:

$$R = \sum_{i=0}^{N} t_{sub} P_{sub,i} + t_{opt} P_{opt,i} \tag{27}$$

Substituting back the expression $t_{opt} = T_{RTO} - t_{sub}$, whereby the time that is not spent operating optimally during the RTO period is spent operating suboptimally instead, both terms can be expressed in terms of the total RTO period length and the suboptimal time:

$$R = \sum_{i=0}^{N} t_{sub} P_{sub,i} + (T_{RTO} - t_{sub}) P_{opt,i} \tag{28}$$

For a single RTO period, equation (28) could be used to build forecasting tools such as payback periods as exemplified in the appendix (supplementary information). If the system were not to act promptly (i.e., be delayed beyond the regular suboptimal time), the time operating suboptimally would be protracted, thus causing diminished economic performance. For instance, suppose the delay incurred at a given RTO period is τ, this causes further suboptimal operating time expressed as:

$$R = \sum_{i=0}^{N} P_{sub,i}(t_{sub,i} + \tau_i) + P_{opt,i}(T_{RTO} - t_{sub,i} - \tau_i) \tag{29}$$

This situation is best avoided as the $T_{RTO} - t_{sub,j} - \tau_i$ term diminishes the potential benefit of an RTO scheme over time. This is especially important in the lv-PE/RTO system as offline computations must be performed before set point updates. As a result, the computational burden, which is associated with the information content procedure must also be considered as to avoid the delay.

The size of M (i.e., the number of samples used for averaging in problems (7) and (19)) will determine whether delay occurs in the proposed lv-PE/RTO scheme through the information content procedure occurring in the PE computer. If M is small, the estimation formulation (7) will not benefit from the smoothing of noise of a large sample size, thus resulting in high variance estimate. In contrast, a large M may capture slow dynamics such as drift or, as noted above, computational delays in the execution of the RTO problem (5). Drift would result in high-error estimates as the data collected would not be dynamic, thus the steady-state estimation problem would aim to fit parameters to dynamic data

using a steady-state model. Computational delays would result in performance deterioration that could become significant if they delay persists over time as shown in equation (29).

The time required to perform $k = j + n_{z_0} - n_z$ sets of challenger problems (as shown in Figure 3), each requiring M samples, depends on the length of the sampling time (Δt) with respect to the CPU time of each challenger problem ($\Delta t_{challenger}$). Whichever time is greater limits the speed of the information content procedure, i.e.,

$$t_{comp} = \begin{cases} kM\Delta t & if & \Delta t > \Delta t_{challenger} \\ kM\Delta t_{challenger} & if & \Delta t_{challenger} > \Delta t \end{cases} \tag{30}$$

In the case studies considered in this work, M was sized based on equation (30) such that the delayed revenue case in represented by equation (29) would be avoided. To do so, it is assumed that $t_{comp} := \Delta T$ such that the maximum allowable computational time (assuming no parallelization, which can also be considered through an integer multiple of equation (30)) was equal to the RTO period, as to avoid any delay. Moreover, $k := n_{z_0}$ was assumed such that all available measurements are assumed to be probed via challenger problems. The time-limiting conditions can be verified through preliminary PE executions, and it was found that $\Delta t > \Delta t_{challenger}$ for both case studies herein (i.e., the sampling period is longer than the computational time to execute a PE problem). Accordingly, the M for each case study was determined by rearranging equation (30) and substituting the aforementioned definitions ($:=$) as follows:

$$M = \frac{\Delta T}{\Delta t n_{z_0}} \tag{31}$$

such that RTO delays are avoided.

Furthermore, the proposed scheme also helps to avoiding constraint violations. To quantify this effect, the sum of absolute constraint violations is considered, i.e.,

$$SAV = \sum_{t=0}^{T_f} |g_{plant,t} - g| \tag{32}$$

where $T_f(time)$ is the total time for which the system is operated while $g_{plant,t}$ and g are the actual (measured) and bound values for the constraints being violated, respectively. The absolute sum is used as it gives a good physical sense of the amount by which the constraint is being exceeded cumulatively over time. SAV preferred to an alternative metric like sum of squares, which also quantifies the violation but does not correspond to an actual plant quantity because of the squaring.

4. Case studies

The proposed scheme was tested for updating the RTO and NMPC parameters as depicted in Figure 1b with matching optimization and control models (however, they need only be passed to one of these layers to influence the process operation). Two simulated case studies are performed: a forced circulation evaporator [28] case exemplifies the benefit of avoiding constraint violations and the Williams-Otto CSTR [29] shows the economic benefit of the lv-PE/RTO scheme. Each case study is tested under different parameter realizations (i.e., where the plant manifests distinct parameter values/combinations) whereby both regular PE and lv-PE schemes must repeatedly estimate the parameters to feed to the RTO and NMPC. The initial conditions (i.e., at $T = 0, t = 0$) for all scenarios within each case study correspond to the optimal operating point given by the nominal parameter(s). Note that this is only the starting point,

and each scheme then proceeds to pursue the true optimum corresponding to the actual parameters for a given scenario. A consistent starting point for both PE/RTO schemes (i.e., the regular and low-variance) and across all scenarios ensures comparability in the dynamic domain such that no scheme/scenario starts at a more advantageous point. As a result, the plant is assumed to have arrived at a new operating point in both case studies, thus progressing through the restart/terminate block in Figure 3, and triggering the measurement-probing block. Both case studies assume full state accessibility as to not confound the performance of the proposed method with the performance of a potential state estimator. Nevertheless, many industrial systems require state estimation for unmeasured states; these estimators (e.g., Kalman filter [3], extended Kalman filter [30], and moving horizon estimation [4,30]) also require noisy process measurements. As the proposed method targets measurement noise, it can be adapted to be compatible with the state estimators and improve the quality of estimates (provided that the system is both identifiable and observable).

In both case studies, the time intervals (i.e., sampling times) are chosen based on literature values [31]. Moreover, the RTO intervals were chosen to be significantly longer than the transient times as to satisfy assumption 1 (section 3). The noise levels are set to be sufficiently high to cause large errors in PE, the minimum number of measurements were based on preliminary tuning experiments, and the sample size M was for each case was determined using equation (31). The proposed scheme will be denoted as "RTO (lv-PE)" while the regular RTO will be denoted as simply "RTO".

The scheme is deployed for various combinations of uncertain parameter(s) as different scenarios within in each case study; the goal of the RTO is to repeatedly estimate the uncertain parameters and operate the system as close to the true optimum as possible. During this time, disturbances were assumed to be measurable and steady as to be able to assess the scheme in the neighbourhood of the optimal operating point and not in large transients; since RTO is a steady state scheme, significant dynamics could confound the analysis. As such, any dynamics observed are owed to set point fluctuations and control actions incited by changing parameter estimates in the RTO and NMPC layers, respectively.

The schemes were assessed on three factors: parameter variability, process cost, and constraint violation (in cases where this occurs). Metrics to quantify these factors are computed *a posteriori* to each simulated case study for both RTO-operated systems with the standard PE and the lv-PE. Firstly, the variability is captured through the standard deviation of parameter estimates computed using formulations (7) and (19). The standard deviation of parameter estimates is central to the proposed approach as it is the main factor effected by the *IC* procedure in section 3.2., which reduces variability using equation (21). As the system is repeatedly estimating parameters for each realization, the variability measures how much these parameters vary by PE execution such that low variability is desired. Secondly, the process economics, which the reduced parameter variability improves upon, are computed through the cumulative process revenue/cost in equation (28) divided by the total operating time of a given scenario. As the system should operate primarily at steady state, this mean process cost should approximate the RTO-optimal steady state cost achieved for each case/scenario. Furthermore, constraint violations can occur as previously mentioned; the cumulative violation is computed using equation (32). As these violations are undesirable, the constraint violation metric used herein is ideally minimized by estimating parameters that yield non-violating set points in the RTO layer.

Both case studies were simulated and optimized in the Pyomo environment, which is a modelling package for PYTHON [32]. Both dynamic simulations were discretized in the time domain using four-point Radau collocations on finite elements per sampling interval. The optimization problems were solved using the MA27 IPOPT solver from the HSL library [33] on an Intel core i7-4770 CPU @ 3.4 GHz.
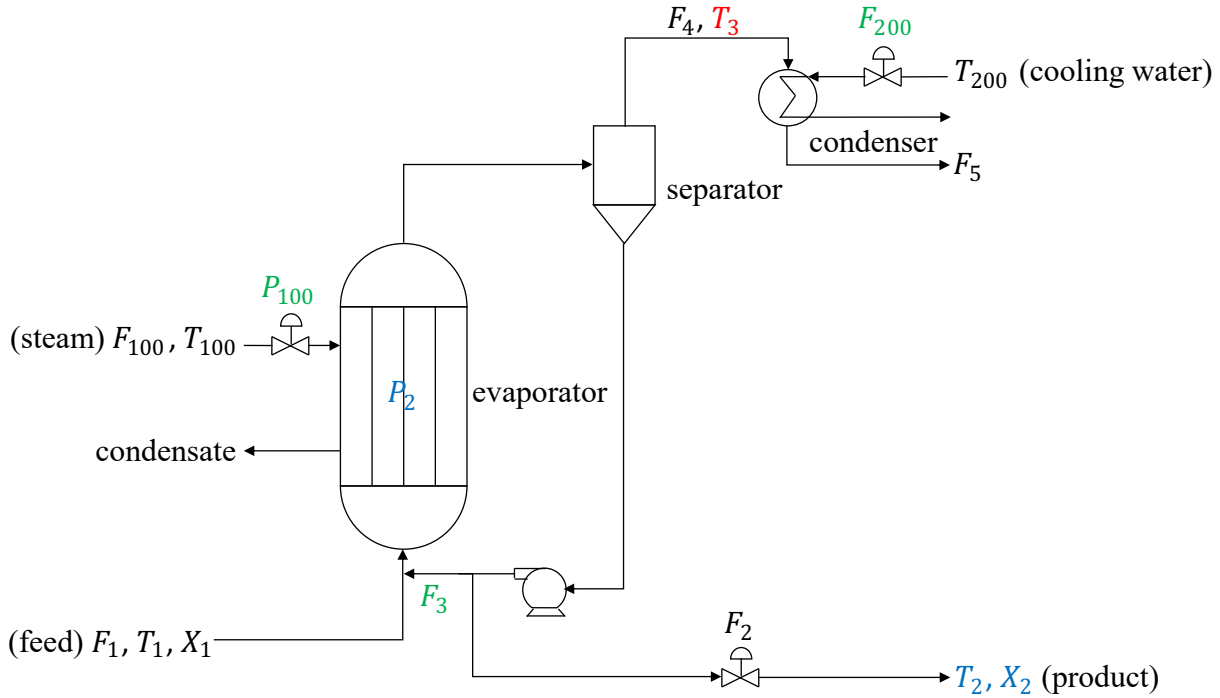
4.1. Forced circulation evaporator

Figure 4: Forced-circulation evaporator process. Blue denotes controlled variables, green denotes manipulated variables, and red denotes additional measurements (i.e., aside from the controlled variables) as implemented in the present study.

The forced circulation evaporator (Figure 4) is a common unit in chemical plants; the mechanistic process model, along with its use in simulation studies, was first introduced by Lee, Newell and Sullivan [28]. The system is of particular interest in the process control literature because of its nonlinearity and many potential control loops owed to the number of possible manipulated/controlled variable pairings [34]. Moreover, the optimal operating point of the system has been observed to occur at an active constraint, hence it provides a good setting in which to investigate the effect of parameter estimates under a potential RTO constraint violation. The evaporator model consists of the following material balances:

$$H \frac{dX_2}{dt} = F_1 X_1 - F_2 X_2 \qquad (33\text{-}1)$$

$$K \frac{dP_2}{dt} = F_4 - F_5 \qquad (33\text{-}2)$$

$$F_2 = F_1 - F_4 \qquad (33\text{-}3)$$

21

where F_1, F_2, F_4, and F_5 (kg/min) are the stream mass flowrates outlined in Figure 4; X_1 and X_2 (%) are the feed and product compositions of the product chemical, respectively, and $P_2 (kPa)$ is the evaporator pressure. Note that the third material balance (33-3) implies a constant mass holdup in the evaporator, which is reflected in the constant holdup term $H(kg)$. The energy balance over the entire process is modelled as follows:

$$T_2 = 0.5616P_2 + 0.3126X_2 + 48.43 \tag{33-4}$$

$$T_3 = 0.507P_2 + 55 \tag{33-5}$$

$$F_4 = \frac{Q_{100} - F_1 C_p (T_2 - T_1)}{\lambda} \tag{33-6}$$

where T_1, T_2, and T_3 (°C) are the stream temperatures as outlined in Figure 4 whereas $Q_{100}(kW)$ is the steam jacket heat duty. The steam jacket energy balance is modelled as follows:

$$T_{100} = 0.1538P_{100} + 90 \tag{33-7}$$

$$Q_{100} = UA_1(T_{100} - T_2) \tag{33-8}$$

$$UA_1 = 0.16(F_1 + F_3) \tag{33-9}$$

$$F_{100} = \frac{Q_{100}}{\lambda_s} \tag{33-10}$$

where $T_{100}(°C)$, $P_{100}(kPa)$, and $F_{100}(kg/min)$ are the saturated steam temperature, pressure, and mass flowrate, respectively. $UA_1(kW/°C)$ is the heat jacket heat transfer coefficient. The condenser is modelled as follows:

$$Q_{200} = \frac{UA_2(T_3 - T_{200})}{1 + \frac{UA_2}{2C_p F_{200}}} \tag{33-11}$$

$$F_5 = \frac{Q_{200}}{\lambda} \tag{33-12}$$

where $T_{200}(°C)$, $Q_{200}(kW)$, and $F_{200}(kg/min)$ are the cooling water temperature, cooling duty, and mass flowrate, respectively. In this case, the manipulated variables are the steam pressure, cooling water flowrate, and recirculation flowrate (i.e., $\boldsymbol{u} = [P_{100} \quad F_{200} \quad F_3]^T$); the controlled variables are the product composition, temperature, and evaporator pressure (i.e., $\boldsymbol{y} = [X_2 \quad P_2 \quad T_2]^T$); the uncertain parameter is the condenser heat transfer coefficient (i.e., $\boldsymbol{\theta} = [UA_2]^T$). The initial measurements are the controlled variables, as well as the separator outlet temperature (i.e., $\boldsymbol{z}_0 = [X_2 \quad P_2 \quad T_2 \quad T_3]^T$). The process losses are to be minimized according to the following objective function:

$$\Phi = P_e(F_2 + F_3) + P_s F_{100} + P_w F_{200} \tag{34}$$

where P_e, P_s, and P_w are the electricity, steam, and cooling water prices, respectively, in Table S1 (supplementary information).

The RTO and NMPC problems (5) and (6) are subject to the following constraints on the controlled variables:

$$25 \leq X_2(\%) \leq 100 \tag{35-1}$$

$$40 \leq P_2(kPa) \leq 80 \tag{35-2}$$

Moreover, the RTO and NMPC problems are also subject to constraints on the manipulated variables:

$$10 \leq P_{100}(kPa) \leq 400 \tag{36-1}$$

$$10 \leq F_{200}(kg/min) \leq 400 \tag{36-2}$$

$$1 \leq F_3(kg/min) \leq 100 \tag{36-3}$$

Lastly, following constraints are imposed on the estimated parameters in problems (7) and (19):

$$0.1 \leq UA_2(kW/°C) \leq 20 \tag{37}$$

Table S1 (supplementary information) presents the model parameters and nominal values used in this study.

The proposed scheme was implemented for this case study using the process model, controlled variables, manipulated variables, constraints, and uncertain parameters described in this section. The system is operated for $833\ h$ with an RTO period of $\Delta T = 16\ hours$ and a sampling interval of $\Delta t = 4\ minutes$. $n_{z,min} = 1$ was chosen based on prior identifiability analysis and the process and measurement noises (w, v; owed to mismatch and instrumentation error, respectively) are additive and zero-mean with 0.1% of the nominal state values as variance $\mathcal{N}(0, (0.001x_{nom})^2)$. The NMPC controller tuning for formulation (5) is $Q = diag(1, 1, 1)$, $R = diag(0.09, 15, 20)$ and $P = C = 200\Delta t$; these are based on preliminary manual tuning to balance tracking speed and stability. Table 1 presents the formulations to the corresponding optimization problems (5), (6), and (7) associated with this case study.

*Table 1: PE, RTO, and NMPC formulations for evaporator case study. *S.S. indicates that a steady-state version of the model is used in the corresponding layer.*

	PE	RTO	NMPC
Objective function	$\|\hat{z} - \bar{z}\|_{K^{-1}}^2$	Eq. (34)	$\sum_{i=1}^{200}\|y_{sp} - \hat{y}_{t+i}\|_Q^2 + \sum_{j=1}^{200}\|\Delta u_{t+j}\|_R^2$
Decision variables	$\theta = [UA_2]^T$	$y = [X_2 \quad P_2 \quad T_2]^T$	$u_{t+1} = [P_{100,t+1} \quad F_{200,t+1} \quad F_{3,t+1}]^T$
Model	Eq. (33). S.S. model	Eq. (33). S.S. model	Eq. (33). Dynamic model
Constraints	Eq. (37)	Eqs. (35)–(36)	Eqs. (35)–(36)
Inputs	$\bar{z} = [\bar{X}_2 \quad \bar{P}_2 \quad \bar{T}_2 \quad \bar{T}_3]^T$ $\bar{u} = [\bar{P}_{100} \quad \bar{F}_{200} \quad \bar{F}_3]^T$ $\bar{d} = [\bar{F}_1 \quad \bar{T}_1 \quad \bar{X}_1]^T$	$\theta = [UA_2]^T$ $d = [F_1 \quad T_1 \quad X_1]^T$	$x_0 = [X_2 \quad P_2]^T$ $y_{sp} = [X_{2,sp} \quad P_{2,sp} \quad T_{2,sp}]^T$ $d_t = [F_{1,t} \quad T_{1,t} \quad X_{1,t}]^T$

The CPU time of each challenger problem is $\sim 0.03\ seconds$, which is significantly less than the sampling time. Accordingly, the sampling time dictates the computational burden of the information content procedure as per equation (30) and the RTO sample size is set to $M = 60$ as per equation (31). All scenarios tested required $k = 4$ sets of challenger problems as shown in Table 2, which corresponds to an actual computational burden of $\sim 3.3\ hours$ (to perform all challenger problems), which is well within the RTO period of 16 $hours$, thus enough data can be collected within the RTO period to perform the information content procedure with no delay.

The uncertain parameter is assumed to materialize in the interval $[(1 - \alpha)\theta_{nom}, (1 + \alpha)\theta_{nom}]$, where $\alpha = 0.1$, for simplicity. The nominal parameter value (corresponding to the initial operating point) can be found in Table S1 (supplementary information). In each scenario, the true plant parameter manifests at a value from the five uniformly spaced points shown in the first row of Table 2. It should be noted that the scheme can be used to estimate any realization of the "true" parameter value; however, the five scenarios in Table 2 were chosen such that they would be representative of the entire uncertain parameter domain while limiting the number of scenarios required for testing.

Table 2: Results for parameter scenarios in the evaporator case study under low-variance and regular RTO implementations.

	Scenario 1 (S1)	Scenario 2 (S2)	Scenario 3 (S3)	Scenario 4 (S4)	Scenario 5 (S5)
$UA_2\ (kW/K)$	$0.9\theta_{nom}$	$0.95\theta_{nom}$	θ_{nom}	$1.05\theta_{nom}$	$1.1\theta_{nom}$
$\sigma_{\theta,lv}\ (K)$	0.67	0.61	0.03	0.28	0.65
$\sigma_{\theta,r}\ (K)$	1.85	1.17	0.82	0.82	2.45
$\bar{P}_{RTO\ (lv-PE)}\ (\$/s)$	272.77	343.11	270.71	270.39	370.00
$\bar{P}_{RTO}\ (\$/s)$	245.20	272.18	303.32	261.73	255.52
$SAV_{RTO\ (lv-PE)}\ (\%)$	2151.51	21310.10	3878.97	5407.98	4023.45
$SAV_{RTO}\ (\%)$	229805.00	186815.60	160069.42	146878.65	179640.75
k	4	4	4	4	4

Figure 5a displays the process losses for several of the scenarios listed in Table 2. It should be observed that the losses and average price rate ($\bar{P}$) in all scenarios (except S3) are lower (i.e., favourable) for the regular RTO implementation than the lv-PE/RTO. This occurs despite the lower variation in the parameter estimates (σ) for all scenarios achieved by the lv-PE/RTO as summarized in Table 2. Figure 5b elucidates that the regular RTO is achieving this decreased cost through violation of the composition constraint in equation (35-1); this is also reflected in substantially lower SAV when the lv-PE/RTO is implemented. The SAV, as defined in equation (32), ranges from one to two orders of magnitude lower when using the lv-PE/RTO than those achieved when using the regular RTO; this results in significant less product being off-specification. The constraint violation occurs as the RTO and NMPC models, which have the estimated parameters, are mismatched from the plant, which has the "true" parameters. Thus, the set points for the RTO and control actions for the NMPC, which appear constraint-abiding in their corresponding optimization

problems, are not so when implemented in the plant. As a result, the better (i.e., lower) price rates of the regular RTO are misleading as the product being produced in the constraint-violating periods will not meet the required specifications. In reality, off-specification product such as that produced in the regular RTO implementation would have to be reprocessed, thereby increasing the processing costs. As the re-processing cost is not considered herein, the regular RTO misleadingly appears to be economically superior in all scenarios (except for S3, where the true parameter was set to their nominal value). In contrast, Figure 5b also shows that the lv-PE/RTO generally operates the plant directly at the constraint and does not vary the set point for X_2 as it does with the set points for T_2 and P_2 as shown in Figure 5c and Figure 5d, respectively. As such, most constraint violation that occurred using the lv-PE/RTO was likely owed to noisy plant fluctuations and not to the proposed parameter estimation scheme.
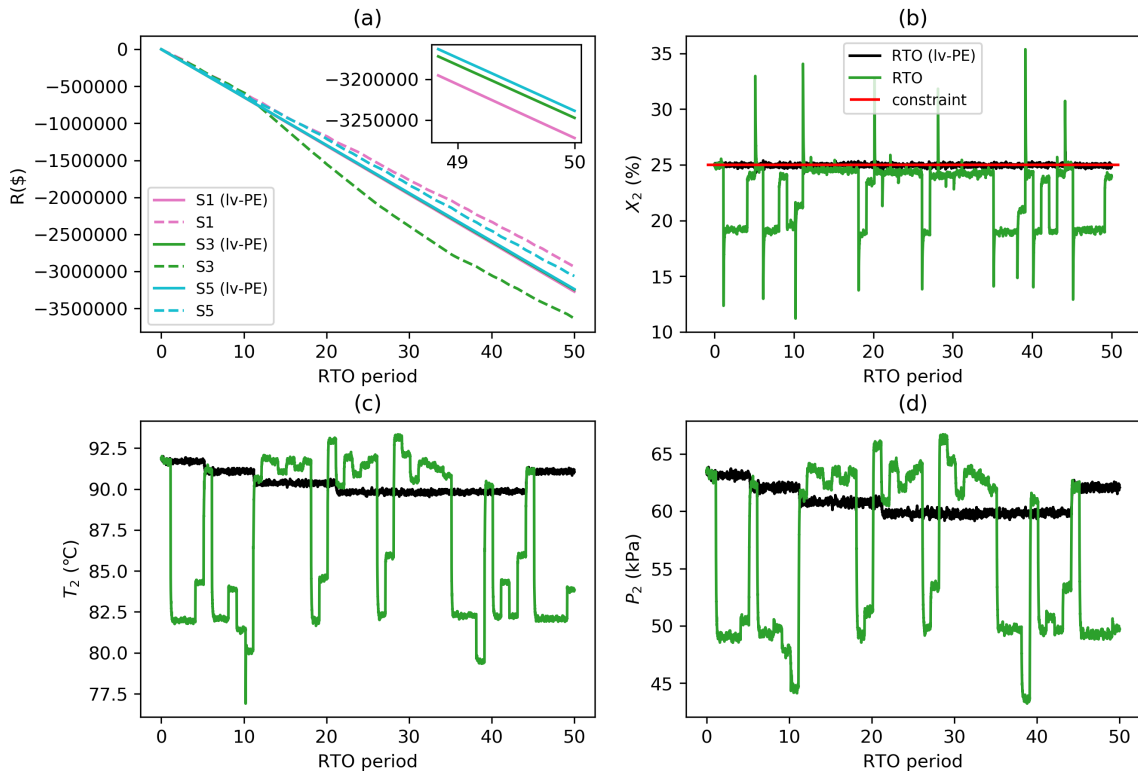

Figure 5: Economics and controlled variables for the evaporator case study. a) losses ($), b) product composition, c) product temperature, d) evaporator pressure.

This variation caused by the parameter on the RTO operation is seen most prominently on Figure 5c and Figure 5d whereby the product temperature and evaporator pressure controlled variables vary when using the regular RTO compared to a significantly more consistent operation produced by the lv-PE/RTO. This variation has a significant impact on the process cost as observed in the sub-window of Figure 5a, where the optimal cost for the lv-PE RTO implementation does not actually vary significantly with respect to the true parameter realizations while the cost of the PE/RTO does despite only a single parameter being assumed to be uncertain in this process. Aside from the constraint violation observed for this case study, the increased variability of the regular RTO also leads to a more active control layer, which is undesirable from an operation and maintenance perspective (not shown for brevity).
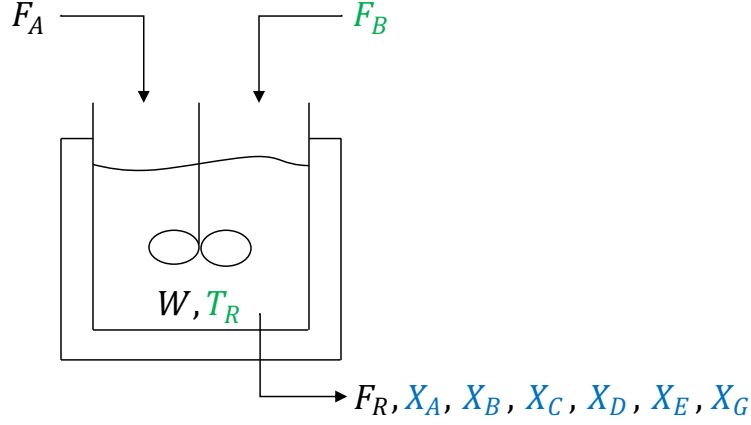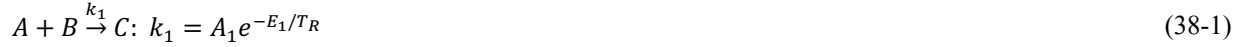
4.2. Williams-Otto CSTR

Figure 6: Williams-Otto CSTR. Blue denotes controlled variables and green denotes manipulated variables as implemented in the present study.

The continuous stirred-tank reactor (CSTR) first described by Williams and Otto [29] is another common system used for real-time optimization and control studies (e.g., [18, 20, 30]). This system has been used as a benchmark example for many economic optimization methods as it provides a relatively small but nonlinear setting that can be used to highlight potential economic improvements. The process is depicted in Figure 6 and consists of two pure inlet streams of substrates A and B with mass flowrates F_A and F_B (kg/s), respectively. While the former flowrate is a disturbance variable, the latter serves as a manipulated variable. Three reactions occur in the system as shown in whereby D and E are the desired products while C and G are intermediate and undesirable biproducts, respectively:

$$A + B \xrightarrow{k_1} C: \; k_1 = A_1 e^{-E_1/T_R} \tag{38-1}$$

$$B + C \xrightarrow{k_2} D + E: \; k_2 = A_2 e^{-E_2/T_R} \tag{38-2}$$

$$C + D \xrightarrow{k_3} G: \; k_3 = A_3 e^{-E_3/T_R} \tag{38-3}$$

where k_1, k_2, and k_3 (s^{-1}) are the reaction rate constants as expressed by the rate laws with pre-exponential factors $(A_1, A_2, A_3(s^{-1}))$ and activation energies $(E_1, E_2, E_3(K))$. The activation energies in this case study are in units of temperature as converted using ideal gas constant. These rate laws depend on the tank temperature $T_R(K)$. The process dynamic and steady state behaviour are modelled using the equations:

$$W \frac{dX_A}{dt} = F_A - F_R X_A - r_1 \tag{38-4}$$

$$W \frac{dX_B}{dt} = F_B - F_R X_B - r_1 - r_2 \tag{38-5}$$

$$W \frac{dX_C}{dt} = -F_R X_C + 2r_1 - 2r_2 - r_3 \tag{38-6}$$

26

$$W\frac{dX_D}{dt} = -F_R X_D + r_2 - 0.5r_3 \tag{38-7}$$

$$W\frac{dX_E}{dt} = -F_R X_E + r_2 \tag{38-8}$$

$$W\frac{dX_G}{dt} = -F_R X_G + 1.5r_3 \tag{38-9}$$

where X_A, X_B, X_C, X_D, X_E, and X_G (kg/kg) are the respective component mass fractions. W (kg) is the mass holdup in the tank, which is assumed to be constant such that the tank material is always at steady state, i.e.,

$$F_R = F_A + F_B \tag{38-10}$$

where the tank outlet flowrate is $F_R(kg/s)$. The reactions proceed according to the substrate concentrations as follows:

$$r_1 = k_1 X_A X_B W \tag{38-11}$$

$$r_2 = k_2 X_B X_C W \tag{38-12}$$

$$r_3 = k_3 X_C X_D W \tag{38-13}$$

where r_1, r_2, and $r_3 (s^{-1})$ are the reaction rates. The manipulated variables for this process are the inlet flowrate of B and tank temperature (i.e., $\boldsymbol{u} = [F_B \quad T_R]^T$). The controlled variables, states, and initial measurements are the component mass fractions (i.e., $\boldsymbol{z}_0 = \boldsymbol{y} = \boldsymbol{x} = [X_A \quad X_B \quad X_C \quad X_D \quad X_E \quad X_G]^T$). The model uncertain parameters considered in this case study are the activation energies (i.e., $\boldsymbol{\theta} = [E_1 \quad E_2 \quad E_3]^T$). The process revenue is to be maximized in this case according to the following objective function:

$$\Phi = P_D F_R X_D + P_E F_R X_E - P_A F_A - P_B F_B - P_T T_R \tag{39}$$

where P_D, P_E, P_A, and P_B are the prices of the products and substrates in Table S2 (supplementary information). The RTO and NMPC problems (5) and (6) are subject to constraints on the controlled variables:

$$0 \le y_i(kg/kg) \le 1 \qquad\qquad \forall i \in \{1, ..., n_y\} \tag{40}$$

Moreover, the RTO and NMPC problems are also subject to constraints on the manipulated variables:

$$2 \le F_B(kg/s) \le 10 \tag{41-1}$$

$$323.15 \le T_R(K) \le 423.15 \tag{41-2}$$

Lastly, following constraints are imposed on the estimated parameters in problems (7) and (19):

$$0.1 \leq E_1, E_2, E_3 (K) \leq 50,000 \tag{42}$$

Table S2 (supplementary information) contains the model parameters and nominal values as used in this study.

The proposed scheme was implemented for the present case study with the model, controlled variables, manipulated variables, constraints and uncertainty parameters described above. The system is operated for $500 \, h$ with an RTO period of $\Delta T = 6.5 \, h$ and a sampling interval of $\Delta t = 3 \, min$. $n_{z,min} = 3$ was determined based on preliminary identifiability analysis and the process and measurement noises $(\boldsymbol{w}, \boldsymbol{v})$ are additive and zero-mean with 10% of the nominal state values as variance $\mathcal{N}(0, (0.1\boldsymbol{x}_{nom})^2)$. The NMPC controller tuning for formulation (5) is $\boldsymbol{Q} = diag(1, 1, 1, 2, 1, 2)$, $\boldsymbol{R} = diag(3, 0.03)$, and $P = C = 10\Delta t$, based on preliminary manual controller tuning. Table 3 presents the formulations to the corresponding optimization problems (5), (6), and (7) associated with this case study.

Table 3: PE, RTO, and NMPC formulations for evaporator case study. *S.S. indicates that a steady-state version of the model is used in the corresponding layer. $S = \{A, B, C, D, E, G\}$ is the set of all species.

	PE	RTO	NMPC
Objective function	$\|\hat{\boldsymbol{z}} - \bar{\boldsymbol{z}}\|_{K^{-1}}^2$	Eq. (39)	$\sum_{i=1}^{10} \|\boldsymbol{y}_{sp} - \hat{\boldsymbol{y}}_{t+i}\|_Q^2 + \sum_{j=1}^{10} \|\Delta \boldsymbol{u}_{t+j}\|_R^2$
Decision variables	$\boldsymbol{\theta} = [E_1 \quad E_2 \quad E_3]^T$	$\boldsymbol{y} = [X_i \forall i \in S]^T$	$\boldsymbol{u}_{t+1} = [F_{B,t+1} \quad T_{R,t+1}]^T$
Model	Eq. (38). S.S. model	Eq. (38). S.S. model	Eq. (38). Dynamic model
Constraints	Eq. (42)	Eqs. (40)–(41)	Eqs. (40)–(41)
Inputs	$\bar{\boldsymbol{z}} = [\bar{X}_i \forall i \in S]^T$ $\bar{\boldsymbol{u}} = [\bar{F}_B \quad \bar{T}_R]^T$ $\bar{\boldsymbol{d}} = [\bar{F}_A]^T$	$\boldsymbol{\theta} = [E_1 \quad E_2 \quad E_3]^T$ $\boldsymbol{d} = [F_A]^T$	$\boldsymbol{x_0} = [X_{i,t} \forall i \in S]^T$ $\boldsymbol{y}_{sp} = [X_{i,sp} \forall i \in S]^T$ $\boldsymbol{d}_t = [F_{A,t}]^T$

In the present case study, each challenger RTO problem required $\sim 0.02 \, s$ to perform and, as with the previous case study, this implies that $\Delta t > \Delta t_{dummy}$. Thus, $M = 20$ according to equation (31) to avoid delays. As stated in Table 4, all scenarios required either $k = 5$ or $k = 6$ sets of challenger problems to be performed, leading to a total computational time of 5 and 6 $hours$ (to perform all challenger problems), respectively. This is within the RTO period time; thus, enough data can be collected, and the challenger problems can be performed with no computational delay to the RTO as determined with equation (31).

Each uncertain parameter is assumed to materialize only at a low (l), nominal (n), and high (h) value in the interval $[(1 - \alpha)\boldsymbol{\theta}_{nom}, (1 + \alpha)\boldsymbol{\theta}_{nom}]$, where $\alpha = 0.1$ and the nominal parameters listed in Table S2 (supplementary information). To the authors' knowledge, this represents the largest parameter uncertainty region to have been considered for the Williams-Otto plant. Hence, a total of 3^3 possible uncertainty scenarios were possible from which the 9 scenarios Table 4 were randomly selected as a representative sample. As with the previous case study, the discretization of the uncertainty was done for simplicity and the proposed scheme can be used to estimate any parameter combination within the aforementioned interval (i.e., it is not limited to any particular set of parameter realizations).

Table 4: Results for parameter combination scenarios in the Williams-Otto case study under low-variance and regular RTO implementations.

	S1	S2	S3	S4	S5	S6	S7	S8	S9
E_1	h	h	n	h	h	l	h	n	n
E_2	n	l	n	h	h	l	l	l	n
E_3	h	l	h	n	h	l	n	h	l
$\sigma_{\theta,lv}$ (K)	99	106	51	59	66	71	201	250	128
$\sigma_{\theta,r}$ (K)	3325	3734	1964	3678	3513	4693	4973	5198	4978
$\bar{P}_{RTO(lv-PE)}$ ($/s$)	2.99	-4.83	5.17	-6.39	-2.40	-1.69	1.21	7.90	-6.33
$\bar{P}_{RTO}$ ($/s$)	2.44	-5.01	5.00	-7.19	-2.77	-3.18	1.01	7.29	-7.51
$\%improvement_{\bar{P}}$	18.39	3.73	3.29	12.52	15.42	88.16	16.53	7.72	18.64
k	6	6	6	5	6	6	6	6	5

Figure 7 displays the process revenue/losses for several non-overlapping scenarios from Table 4 calculated using equation (28). As can be observed, the parameter combination affects whether the process will operate at a revenue or loss; the Williams-Otto plant is only profitable in some cases. Nevertheless, the lv-PE/RTO always results in a more economical operation. This is reflected in the average profit rates ($\bar{P}$) for both schemes as shown in Table 4 whereby the lv-PE/RTO has lower average rates in all scenarios as quantified in the %improvement. These improved economics are a result of the decreased variation in the parameter estimates over the 80 RTO periods analyzed, which are observed to generally have decreased by one or two orders of magnitude as per the σ values in Table 4. Depending on the parameter combination, the lv-PE/RTO can lead to modest (e.g., 3.28% for S3) or significant (e.g., 88.16% for S6) improvements on revenue/loss with respected to the regular RTO.
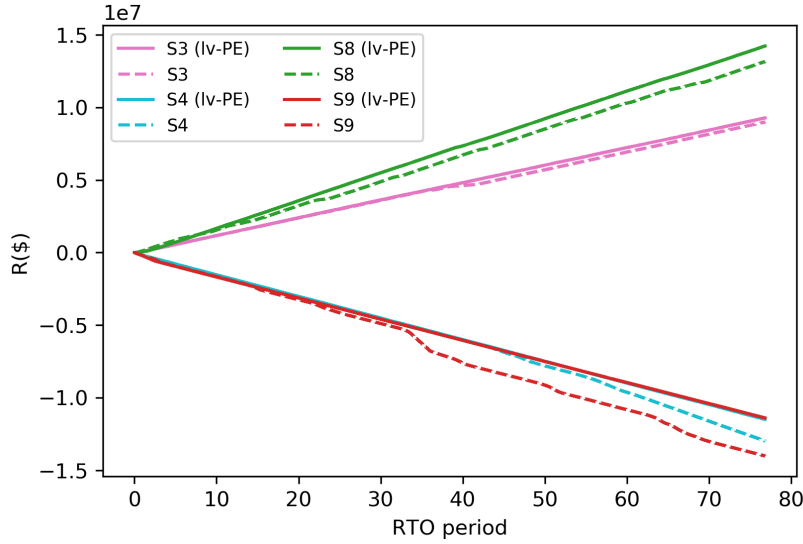
Figure 7:Revenue/loss ($) for several of the scenarios in the Williams-Otto case study.

The effect of variance manifests most directly on the manipulated variables, as shown for S8 and S9 in Figure 8 and Figure 9, respectively. Figure 8 exemplifies the effect that measurement noise has on the NMPC and RTO via the parameter updates in an operating scenario without active constraints. As displayed therein, both manipulated variables have brief spikes that correspond to the cases when parameters and set points are changed through execution of the PE and RTO. This is primarily due to the sudden change in controller parameters, which momentarily sends the system on a transient, but also corresponds to small set point corrections. These spikes were observed to be significantly smaller for the lv-PE/RTO than the regular RTO; the resulting transients, which are shorter when the lv-PE/RTO is employed, ensure that the system operates near its optimum for a longer period, thus improving economic performance. The lv-PE/RTO can be observed to result in a far more consistent performance, thus damping the effect of the noisy measurements on the scheme. Figure 9 is an atypical scenario where the optimal operating policy occurs at the lower bounds of the manipulated variables in equation (41); however, this further elucidates how the lv-PE/RTO can maintain the system at its bound with smaller and less frequent deviations. Another consequence observed therein is the effect of the filter-step of the lv-PE/RTO to avoid periods where the system is operating at non-optimal points. This is also observed between $T = 30$ and $T = 40$ in Figure 9 whereby both manipulated variables are not operating at their bounds (i.e., the economic optimum); meaning that the regular RTO was passed an significantly suboptimal set of set points and parameters, which did not reflect the current operating conditions.
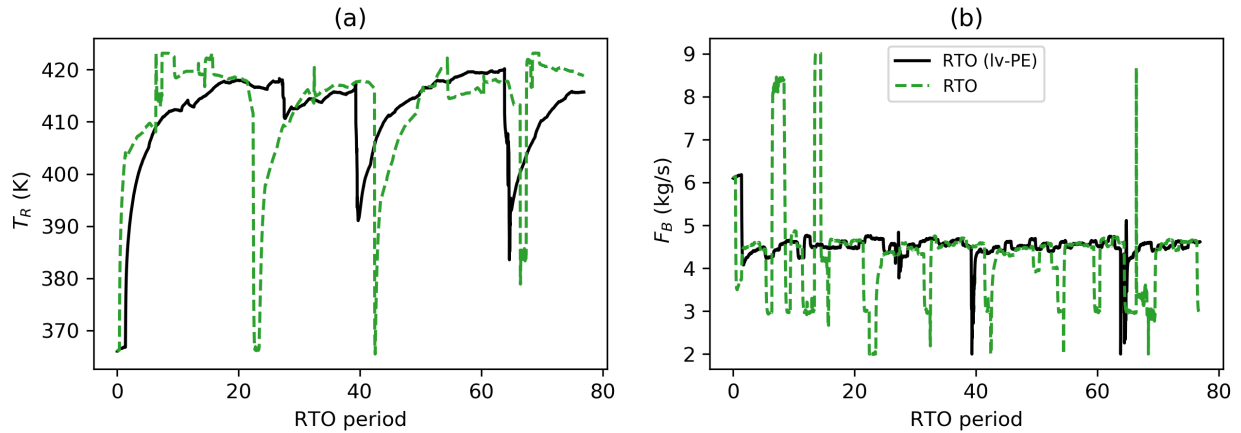
Figure 8: Manipulated variables for S8 of the Williams-Otto case study under the lv-PE/RTO and the regular RTO implementations. (a) reactor temperature, (b) inlet flowrate of substrate "B".
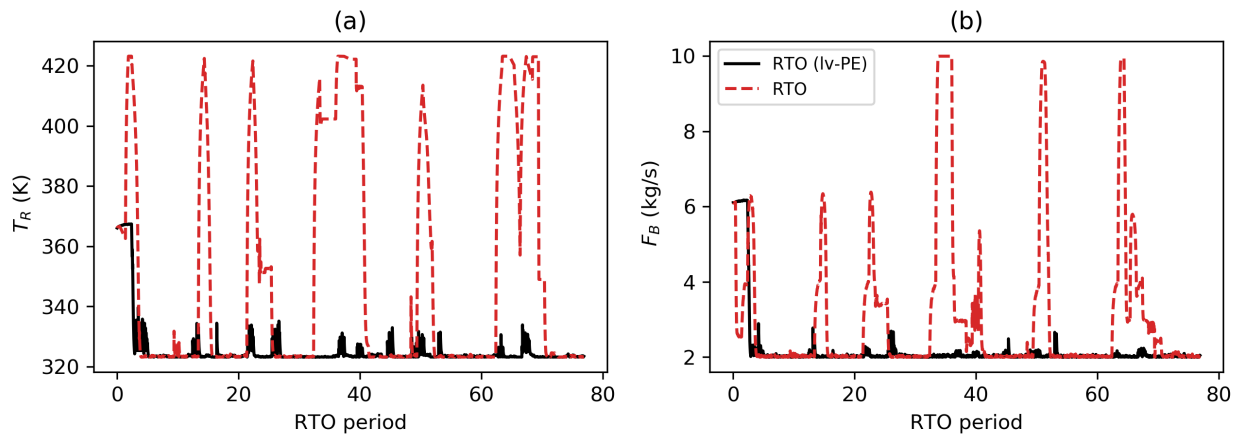

Figure 9: Manipulated variables for S9 of the Williams-Otto case study under the lv-PE/RTO and the regular RTO implementations. (a) reactor temperature, (b) inlet flowrate of substrate "B".

Figure 10 provides contours of the process profit rates (i.e., $\$/time$) for S8 and S9. These were constructed using the true plant parameters such that they are the "true" profit rate contours. Since these are the "true" contours that correspond to the true parameters in S8 and S9, the performance of the PE scheme can be assessed by how closely they approach the top elevations therein. If the steady-state combinations of manipulated variables are treated as a sampled quantity, the confidence ellipsoids for these manipulated variables in both regular RTO and lv-PE/RTO can be constructed. By superimposing these ellipsoids on the contours, the precision and accuracy of the PE schemes is visualized through the size and closeness to the true optimum, respectively. Figure 10 shows these ellipses being centered in the contour region with the most economical profit rates as per the black-shaded elevations, this confirms that the RTO is indeed operating generally near the optimum. However, in both scenarios, the confidence ellipse for the lv-PE/RTO can be observed to be inside the confidence ellipse for the regular RTO; this confirms that the variance in the steady-state manipulated variables has decreased, and in some cases by a significant amount (e.g., S9). The statistical interpretation follows that if many difference samples were taken to replicate the construction of the ellipses, then 95% of the constructed ellipses would contain the mean; as such small ellipses imply lower variation in the

sampled quantities — in this case, the manipulated variables. Accordingly, the improvement in process economics occurs through this decrease in variation.
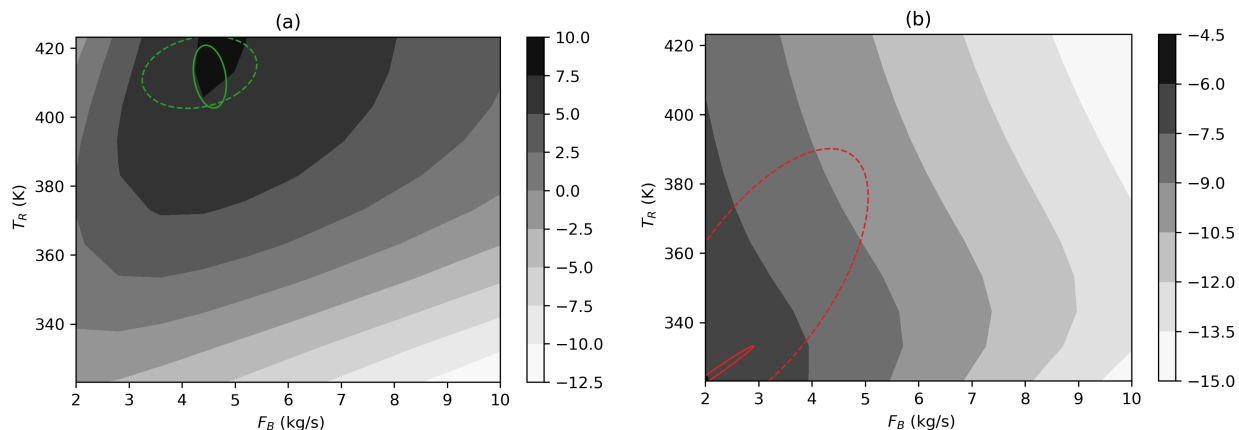

Figure 10: Contour plots with the process profit rates ($/s) on the elevations and manipulated variables on the axes for the Williams-Otto case. (a) S8, (b) S9. 95% confidence ellipsoids shown for the manipulated variables under the regular RTO (dashed lines) and lv-PE/RTO (solid lines).

5. Conclusion and future works

Noisy measurements and model uncertainty are inevitable when operating chemical processes, which may lead to poor RTO performance. As RTO attempts to address model uncertainty by adapting model parameters, noisiness can propagate to these parameter estimates leading to poor process performance. This study presents a novel low-variance parameter estimation (lv-PE) scheme applied to RTO for noisy processes. The proposed scheme uses the information content (IC) metric, as well as establishing parameter bounds for filtering; these novelties reduce the variability in parameter estimates over time and eliminates poorly estimated parameters, respectively. The scheme is motivated through an analysis of RTO economics as affected by set point error owed to parameter inaccuracy. Moreover, the potential computational cost of the scheme is analyzed to avoid any delays are incurred as a result. The proposed scheme was implemented in two case studies, namely a forced circulation evaporator and the Williams-Otto CSTR. The evaporator displayed the ability of the proposed scheme to avoid constraint violations by one to two orders in magnitude, while the Williams-Otto case study showed the improvement yielded by the proposed scheme on process economics ranging from ~4 to 88%, depending on the scenario. Although the benefit provided by the lv-PE to each case study was different, both were observed to result in significant reduction in parameter variation owing to the lv-PE/RTO of one to two orders of magnitude.

Despite the positive results observed herein, some aspects of the lv-PE/RTO remain to be investigated. Namely, both case studies observed herein have fast dynamics and were assumed to be sampled frequently; indeed, this is a key feature in the motivation of the method. A future research avenue could observe the impact of the lv-PE/RTO in slower systems, which will take longer to perform the information content procedure. Conversely, the effects of variation in parameters could be more pronounced as slower system could be operating suboptimally for longer periods of time. Similarly, both systems in this study featured relatively small models that could be solved quickly to also facilitate the information content procedure (i.e., execution of the challenger problems). In the future, the proposed scheme should also be tested in larger systems where the models are less parsimonious causing delays in the lv-PE/RTO. Additionally,

the parameter update effect on model-based state estimators (e.g., moving horizon estimation) should also be explored. Alternatively, the concept of IC to pre-process measurements and generate parameter bounds could be adapted for a state, parameter, or disturbance estimation procedure (or a joint estimation procedure). Moreover, the respective estimators could also be adapted as dynamic problems to address issues such as parameter drift or frequent unmeasurable disturbances. Finally, as noted previously, another direction for future work is the extension of the current methodology for joint estimation variance reduction and GED.

Supporting information

Appendices and model parameter/pricing information are included in the supplement. This information is available free of charge via the Internet at http://pubs.acs.org/.

References

[1] Darby ML, Nikolaou M, Jones J, Nicholson D. RTO: An overview and assessment of current practice. *J. Process Control*, 21(6), 874–884 (2011). https://doi.org/10.1016/j.jprocont.2011.03.009.

[2] Navia D, Villegas D, Cornejo I, de Prada C. Real-time optimization for a laboratory-scale flotation column. *Comput. Chem. Eng.*, 86, 62–74 (2016). https://doi.org/10.1016/j.compchemeng.2015.12.006.

[3] Patrón GD, Ricardez-Sandoval L. Real-Time Optimization and Nonlinear Model Predictive Control for a Post-Combustion Carbon Capture Absorber. *IFAC-PapersOnLine*, 53(2), 11595–11600, (2020). https://doi.org/10.1016/j.ifacol.2020.12.639.

[4] Patrón GD, Ricardez-Sandoval L. An integrated real-time optimization, control, and estimation scheme for post-combustion CO_2 capture. *Appl. Energy*, 308, 118302 (2022). https://doi.org/10.1016/j.apenergy.2021.118302.

[5] Galan A, de Prada C, Gutierrez G, Sarabia D, Grossman IE, Gonzales R. Implementation of RTO in a large hydrogen network considering uncertainty. *Optim. Eng.*, 20, 1161–1190 (2019). https://doi.org/10.1007/s11081-019-09444-3.

[6] Krasławski A. Review of various types of uncertainty in chemical engineering. *Chem. Eng. Process.*, 26(3), 185–191 (1989). https://doi.org/10.1016/0255-2701(89)80016-9.

[7] Marchetti A, Chachuat B, Bonvin D. Modifier-Adaptation Methodology for Real-Time Optimization. *Ind. Eng. Chem. Res., 48, 6022*–6033 (2009). https://doi.org/10.1021/ie801352x.

[8] Roberts PD, Williams TW. On an algorithm for combined system optimisation and parameter estimation. *Automatica*, 17(1), 199–209 (1981). https://doi.org/10.1016/0005-1098(81)90095-9.

[9] Cox H. On the Estimation of State Variables and Parameters for Noisy Dynamic Systems. *IEE Trans. Automat. Contr.*, 9(1), 5–12 (1964). 10.1109/TAC.1964.1105635.

[10] Cao S, Rhinehart RR. An efficient method for on-line identification of steady state. *J. Process Control*, 5(6), 363–374 (1995). https://doi.org/10.1016/0959-1524(95)00009-F.

[11] Özyurt DB, Pike RW. Theory and practice of simultaneous data reconciliation and gross error detection for chemical processes. *Comput. Chem. Eng.*, 28(3), 381–402 (2004). https://doi.org/10.1016/j.compchemeng.2003.07.001.

[12] Bhat SA, Saraf DN. Steady-State Identification, Gross Error Detection, and Data Reconciliation for Industrial Process Units. *Ind. Eng. Chem. Res.*, 43, 4323–4336 (2004). https://doi.org/10.1021/ie030563u.

[13] Arora N, Biegler LT. Redescending estimators for data reconciliation and parameter estimation. *Comput. Chem. Eng.,* 25(11), 1585–1599 (2001). https://doi.org/10.1016/S0098-1354(01)00721-9.

[14] Yuan Y, Khatibisepehr S, Huang B, Li Z. Bayesian Method for Simultaneous Gross Error Detection and Data Reconciliation. *AIChe J.*, 68(3), 3232–3248 (2015). https://doi.org/10.1002/aic.14864.

[15] Albuquerque JS, Biegler LT. Data reconciliation and gross-error detection for dynamic systems. *AIChE J.,* 42(10), 2841–2856 (1996). https://doi.org/10.1002/aic.690421014.

[16] Quelhas AD, de Jesus NJC, Pinto JC. Common vulnerabilities of RTO implementations in real chemical processes. *Can. J. Chem. Eng.,* 91(4), 652–668 (2013). https://doi.org/10.1002/cjce.21738

[17] Zhang Y, Monder D, Forbes JF. Real-time optimization under parametric uncertainty: a probability constrained approach. *J. Process Control*, 12(3), 373–389 (2002). https://doi.org/10.1016/S0959-1524(01)00047-6.

[18] Miletic IP, Marlin TE. On-line Statistical Results Analysis in Real-Time Operations Optimization. *Ind. Eng. Chem. Res*., 37(9), 3670–3684 (1998). https://doi.org/10.1021/ie9707376.

[19] Liu J, Gnanasekar A, Zhang Y, Bo S, Liu J, Hu J, Zou T. Simultaneous State and Parameter Estimation: The role of Sensitivity Analysis. *Ind. Eng. Chem. Res*., 60, 2971–2982 (2021). https://doi.org/10.1021/acs.iecr.0c03793.

[20] Matias JOA, Le Roux GAC. Real-time optimization with persistent parameter adaptation using online parameter estimation. *J. Process Control*, 68, 195–204 (2018). https://doi.org/10.1016/j.jprocont.2018.05.009.

[21] Krishnamoorthy D, Foss B, Skogestad S. Steady-state real-time optimization using transient measurements. *Comput. Chem. Eng.,* 115, 34–45 (2018). https://doi.org/10.1016/j.compchemeng.2018.03.021.

[22] Valluru J, Patwardhan SC. An Integrated Frequent RTO and Adaptive Nonlinear MPC Scheme Based on Simultaneous Bayesian State and Parameter Estimation. *Ind. Eng. Chem. Res*., 58(18), 7561–7578 (2019). https://doi.org/10.1021/acs.iecr.8b05327.

[23] Adetola V, Guay M. Integration of real-time optimization and model predictive control. *J. Process Control*, 20(2), 125–133 (2010). https://doi.org/10.1016/j.jprocont.2009.09.001.

[24] Diehl M, Bock HG, Schlöder JP, Findeisen R, Nagy Z, Allgöwer F. Real-time optimization and nonlinear model predictive control of processes governed by differential-algebraic equations. *J. Process Control*, 12(4), 577–585 (2002). https://doi.org/10.1016/S0959-1524(01)00023-3.

[25] Vrugt JA, Bouten W, Weerts AH. Information Content of Data for Identifying Soil Hydraulic Parameters from Outflow Experiments. *Soil Sci. Soc. Am. J*., 65(1), 19–27 (2001). https://doi.org/10.2136/sssaj2001.65119x.

[26] Kravaris C, Hahn J, Chu Y. Advanced and selected recent developments in state and parameter estimation. *Comput. Chem. Eng.,* 51, 111–123 (2013). https://doi.org/10.1016/j.compchemeng.2012.06.001.

[27] Guillaume JHA, Jakeman JD, Marsili-Libelli S, Asher M, Brunner P, Croke B, Hill MC, Jakeman AJ, Keesman KJ, Razavi S, Stigter JD. Introductory overview of identifiability analysis: A guide to evaluating whether you have the right type of data for your modeling purpose. *Environ. Model. Softw.,* 119, 418–432 (2019). https://doi.org/10.1016/j.envsoft.2019.07.007.

[28] Lee PL, Newell RB, Sullivan GR. Generic Model Control – A Case Study. *Can. J. Chem. Eng*., 67, 478–484 (1989). https://doi.org/10.1002/cjce.5450670320.

[29] Williams TJ, Otto RE. A generalized chemical process model for the investigation of computer control. *IEEE Trans. Commun*., 79(5), 458–473 (1960). 10.1109/TCE.1960.6367296.

[30] Valipour M, Ricardez-Sandoval LA. Assessing the Impact of EKF as the Arrival Cost in the Moving Horizon Estimation under Nonlinear Model Predictive Control. *Ind. Eng. Chem. Res*., 60(7), 2994–3012 (2021). https://doi.org/10.1021/acs.iecr.0c06095.

[31] Amrit R, Rawlings JB, Biegler LT. Optimizing process economics online using model predictive control. *Comput. Chem. Eng.,* 58, 334–343 (2013). https://doi.org/10.1016/j.compchemeng.2013.07.015

[32] Hart W, Watson J, Woodruff D. Pyomo: modeling and solving mathematical programs in Python. *Math. Program Comput.*, 3(3), 219–260 (2011). https://doi.org/10.1007/s12532-011-0026-8.

[33] HSL. A collection of Fortran codes for large scale scientific computation. http://www.hsl.rl.ac.uk.

[34] Govatsmark MS, Skogestad S. Control structure selection for an evaporation process. *Comput. Aided Chem. Eng.,* 9, 657–662 (2001). https://doi.org/10.1016/S1570-7946(01)80104-8.

TOC/Abstract graphic

$$[\overline{\boldsymbol{\theta}} - \boldsymbol{\sigma}_{\theta(\mathbf{z})}, \overline{\boldsymbol{\theta}} + \boldsymbol{\sigma}_{\theta(\mathbf{z})}]$$

$$IC_{i,k} = 1 - \frac{\sigma_{\theta(\zeta),i,k}}{\sigma_{\theta(\mathbf{z}),i,k}} \quad \forall i \in \{1, \dots, n_\theta\}$$

parameter variability reduction

Steady-state process profit